

# 1 **Title: SARS-CoV-2 correlates of protection from infection against** 2 **variants of concern**

3 **Author list:** Kaiyuan Sun<sup>1†\*</sup>, Jinal N. Bhiman<sup>2,3†</sup>, Stefano Tempia<sup>4,5,6</sup>, Jackie Kleynhans<sup>4,5</sup>,  
4 Vimbai Sharon Madzorera<sup>2,3</sup>, Qiniso Mkhize<sup>2,3</sup>, Haajira Kaldine<sup>2,3</sup>, Meredith L McMorro<sup>6,8</sup>,  
5 Nicole Wolter<sup>4,7</sup>, Jocelyn Moyes<sup>4,5</sup>, Maimuna Carrim<sup>4,7</sup>, Neil A Martinson<sup>9,10</sup>, Kathleen Kahn<sup>11</sup>,  
6 Limakatso Lebina<sup>9</sup>, Jacques D. du Toit<sup>11</sup>, Thulisa Mkhencele<sup>4</sup>, Anne von Gottberg<sup>4,7</sup>, Cécile  
7 Viboud<sup>1‡</sup>, Penny L. Moore<sup>2,3,12‡</sup>, Cheryl Cohen<sup>4,5‡\*</sup> for the PHIRST-C group<sup>#</sup>

## 8 **Affiliations:**

9 <sup>1</sup>Division of International Epidemiology and Population Studies, Fogarty International Center, National  
10 Institutes of Health, Bethesda, Maryland, United States of America.

11 <sup>2</sup>SAMRC Antibody Immunity Research Unit, University of the Witwatersrand, Johannesburg, South  
12 Africa

13 <sup>3</sup>Centre for HIV and STIs, National Institute for Communicable Diseases of the National Health  
14 Laboratory Service, Johannesburg, South Africa

15 <sup>4</sup>Centre for Respiratory Diseases and Meningitis, National Institute for Communicable Diseases of the  
16 National Health Laboratory Service, Johannesburg, South Africa.

17 <sup>5</sup>School of Public Health, Faculty of Health Sciences, University of the Witwatersrand, Johannesburg,  
18 South Africa.

19 <sup>6</sup>Influenza Division, Centers for Disease Control and Prevention, Atlanta, Georgia, United States of  
20 America.

21 <sup>7</sup>School of Pathology, Faculty of Health Sciences, University of the Witwatersrand, Johannesburg, South  
22 Africa.

23 <sup>8</sup>COVID-19 Response, Centers for Disease Control and Prevention, Atlanta, Georgia, United States.

24 <sup>9</sup>Perinatal HIV Research Unit, University of the Witwatersrand, South Africa.

25 <sup>10</sup>Johns Hopkins University Center for TB Research, Baltimore, Maryland, United States of America.

26 <sup>11</sup>MRC/Wits Rural Public Health and Health Transitions Research Unit (Agincourt), School of Public  
27 Health, Faculty of Health Sciences, University of the Witwatersrand, Johannesburg, South Africa.

28 <sup>12</sup>Centre for the AIDS Programme of Research in South Africa (CAPRISA), Durban, South Africa

29 †These authors contributed equally.

30 ‡These authors jointly supervised this work.

31 \*Corresponding authors. Email: kaiyuan.sun@nih.gov (KS); cherylc@nicd.ac.za (CC)

32 # A list of authors and their affiliations appears at the end of the paper.

33

34

## 35 **Abstract**

36 Serum neutralizing antibodies (nAbs) induced by vaccination have been linked to protection  
37 against symptomatic COVID-19 and severe disease. However, much less is known about the  
38 efficacy of nAbs in preventing the acquisition of infection, especially in the context of natural  
39 immunity and against SARS-CoV-2 immune-escape variants. In this study, we conducted  
40 mediation analysis to assess serum nAbs induced by prior SARS-CoV-2 infections as potential  
41 correlates of protection (CoPs) against Delta and Omicron BA.1/2 wave infections, in rural and  
42 urban household cohorts in South Africa. We find that, in the Delta wave, anti-D614G nAbs  
43 mediate 37% (95%CI 34% – 40%) of the total protection against infection conferred by prior  
44 exposure to SARS-CoV-2, and that protection decreases with immunity waning. In contrast, anti-  
45 Omicron BA.1 nAbs mediate 11% (95%CI 9 – 12%) of the total protection against Omicron  
46 BA.1/2 wave infections, due to Omicron’s neutralization escape. These findings underscore that  
47 CoPs mediated through nAbs are variant-specific, and that boosting of nAbs against circulating  
48 variants might restore or confer immune protection lost due to nAb waning and/or immune  
49 escape. However, the majority of immune protection against SARS-CoV-2 conferred by natural  
50 infection cannot be fully explained by serum nAbs alone. Measuring these and other immune  
51 markers including T-cell responses, both in the serum and in other compartments such as the  
52 nasal mucosa, may be required to comprehensively understand and predict immune protection  
53 against SARS-CoV-2.

54

## 55 Main text

56 The acute phase of the COVID-19 pandemic has waned with the development of SARS-CoV-2  
57 population immunity in most individuals through repeated episodes of vaccination, infection, or  
58 both <sup>1,2</sup>. Owing to the unprecedented speed of SARS-CoV-2 vaccine development and  
59 distribution <sup>3</sup>, considerable numbers of people were primed by vaccination, averting substantial  
60 morbidity and mortality <sup>4</sup>. However, due to immune evasive variants, vaccine hesitancy, and lack  
61 of global equity in vaccine access <sup>5-7</sup>, a substantial proportion of the world's population acquired  
62 SARS-CoV-2 immunity through natural infections, especially in low- and middle-income  
63 countries <sup>8,9</sup>. Immune markers that reliably predict protection from infection or symptomatic  
64 disease are known as “correlates of protection” (CoP). The post-pandemic era is marked by rapid  
65 antigenic drift of Omicron subvariants leading to continued immune evasion <sup>10-13</sup>. Given this  
66 complex evolutionary landscape, it remains important to identify CoPs induced by natural  
67 infections and/or vaccinations against SARS-CoV-2 variants to monitor population  
68 susceptibility, anticipate future waves, optimize rollout of existing vaccines, and facilitate design  
69 and approval of next generation vaccines <sup>14</sup>. There has been significant progress in defining  
70 serum neutralizing or binding antibodies to the spike protein as CoPs for COVID-19 vaccines,  
71 although most of the data are derived from early randomized controlled trials focused on peak  
72 immune response shortly after vaccination and measured against symptomatic disease caused by  
73 the ancestral strain, with updated data on variants <sup>15-24</sup>. In comparison, little is known about  
74 serum CoPs for infection-induced immunity and protection against acquisition of subclinical  
75 infections.

76 CoPs may differ for immunity induced by infection vs. vaccination: SARS-CoV-2 infections  
77 tend to induce more robust mucosal immunity despite lower serum antibody responses than  
78 intramuscularly delivered mRNA vaccines, as shown in on a mouse model <sup>25</sup>, and mucosal  
79 immunity may play a more important role in reducing risk of infection and transmission than  
80 systemic immunity <sup>26,27</sup>. Moreover, CoPs need to be interpreted in the context of viral evolution:  
81 in the pre-Omicron era, SAR-CoV-2 variants of concerns emerged independently from one  
82 another, with the Alpha, Beta, Gamma, Delta, and Omicron variants exhibiting distinct  
83 phenotypic characteristics. The Omicron variant stands out due to substantial genetic divergence  
84 from earlier strains and significant immune evasion capabilities against antibody neutralization

85 <sup>28</sup>. Equivalent antibody titers may not provide equivalent levels of protection against ancestral  
86 strains compared to more transmissible and immune-evasive variants like Omicron, and CoPs  
87 may therefore be variant-dependent. Furthermore, serum antibody titers against SARS-CoV-2  
88 also wane with time.

89 The challenge of defining CoP for infection induced immunity partially stems from the  
90 difficulty of tracking immune exposures to SARS-CoV-2 infections, given that a significant  
91 proportion of infections are asymptomatic or subclinical and cannot be fully captured by  
92 traditional symptom-based surveillance protocols. The SARS-CoV-2, influenza, and respiratory  
93 syncytial virus community burden, transmission dynamics, and viral interaction in South Africa  
94 (PHIRST-C) cohorts in South Africa <sup>29,30</sup> overcame this challenge by implementing a rigorous  
95 sampling strategy, including collection of nasal swabs twice-weekly during a period of intense  
96 follow up, along with a total of 10 sequential blood draws spanning the D614G, Beta, Delta, and  
97 Omicron BA.1/2 waves. This high-intensity sampling scheme allowed us to reconstruct the  
98 cohort participants' SARS-CoV-2 infection histories with high fidelity, and to monitor infection-  
99 induced antibody responses over time <sup>30</sup>. Blood samples collected immediately prior to Delta and  
100 Omicron waves offered a unique opportunity to investigate serum immune marker levels in close  
101 proximity to the next SARS-CoV-2 exposure. Furthermore, vaccine-derived immunity remained  
102 low at the onset of the Omicron BA.1/2 wave, with less than 25% of the population fully  
103 immunized with Ad26.COV2.S (Janssen) and/or BNT162b2 (Pfizer BioNTech) vaccines <sup>31</sup>. In  
104 this study, we leveraged the PHIRST-C cohorts' unique serological and epidemiological data to  
105 perform mediation analysis and assess neutralizing antibody (nAb) titers induced by prior  
106 infection as CoPs against variants of concerns. Specifically, we evaluated the role of anti-D614G  
107 and anti-Omicron BA.1 nAbs against the Delta and Omicron BA.1/2 variants.

108

## 109 **Results**

### 110 **Cohort description and antibody titer measurements**

111 We analyzed data from the multi-year PHIRST-C cohort study, covering the first four waves of  
112 SARS-CoV-2 infections including the Delta and Omicron BA.1/2 waves <sup>29,30</sup>. The study included  
113 a rural and an urban site in two provinces of South Africa. A total of 1200 individuals from 222  
114 randomly selected households among the two study sites were longitudinally followed from June

115 2020 through April 2022. The study was characterized by intense nasopharyngeal swab and  
116 serum sample collection from the peak of the SARS-CoV-2 D614G (1<sup>st</sup>) wave to after the peak  
117 of the Delta (3<sup>rd</sup>) wave. After this initial follow-up period, nasopharyngeal swab sample  
118 collection stopped but serum samples continued with blood drawn immediately following the  
119 Omicron BA.1/2 (4<sup>th</sup>) wave. The timing of the serum sample collection is visualized in Fig. 1.  
120 We previously reconstructed the detailed SARS-CoV-2 infection history of each individual in the  
121 cohort up to the Omicron BA1/2 wave and demonstrated that immunity conferred by prior  
122 infection reduced the risk of reinfection<sup>30,32</sup>. In this study, we extended this work to investigate  
123 how infection-induced neutralizing antibody (nAb) titers correlate with protection against SARS-  
124 CoV-2 reinfection with the Delta or Omicron BA.1/2 variants.

125 For the Delta wave, we focused on a subgroup of 797 participants from 196 households (Delta  
126 wave subgroup, Table 1, Extended Data Fig. 1) who remained SARS-CoV-2 naïve or had a  
127 single prior SARS-CoV-2 infection before the Delta wave (hence, removing vaccinated and  
128 repeatedly infected individuals from the analysis; see Fig. 1 for the timing of the Delta wave).  
129 We define prior infection as positivity on the Roche Elecsys anti-nucleocapsid assay (an assay  
130 was optimized to detect prior infection<sup>33</sup>), and/or rRT-PCR-positivity, at or before blood draw 5  
131 (refer to BD5 hereafter). SARS-CoV-2 infections during the Delta wave were inferred based on  
132 the anti-nucleocapsid antibody level of two pre- and one post- Delta wave serum samples, as  
133 previously described<sup>30</sup>. We focused on households with no more than six infected household  
134 members during this wave, due to computational constraints of the transmission model (see  
135 Methods Section 4 for details). Among the 797 subgroup participants, 34% (273/797) were  
136 infected during the Delta wave, with attack rates of 42% (229/544) and 17% (44/253) for naïve  
137 and previously infected participants, respectively.

138 To identify CoPs against the Delta variant, for the 797 participants who had been previously  
139 infected, we measured their anti-D614G nAb titers (measured as the inhibitory dilution at which  
140 50% neutralization is attained, referred to as ID<sub>50</sub> hereafter), using the blood draw immediately  
141 preceding the Delta wave (BD5). To evaluate the potential impact of antibody waning, we also  
142 measured the peak nAb level for each participant (defined as the highest anti-D614G nAb titer  
143 among the first 5 blood draws). We then calculated the degree to which nAbs had waned from  
144 peak level to that at BD5 by calculating the difference between peak nAb titer and nAb titer at  
145 BD5 (denoted as  $\Delta nAb^W$  hereafter). If the peak response was already below the nAb assay

146 detection threshold (which is set at 20), then  $\Delta nAb^W$  was also assigned to be below the  
147 threshold, since further titer drop was not detectable. Notably, 28% (32/113) and 58% (81/140)  
148 of individuals previously infected with D614G and Beta exhibited anti-D614G nAb titers below  
149 the detection threshold at BD5, respectively (Extended Data Table 1). The proportion below the  
150 detection threshold was higher for individuals previously infected with the Beta variant than the  
151 D614G variant, given the Beta variant has eight amino acid difference in the spike, resulting in  
152 an antigenically distinct receptor binding domain compared to the D614G variant used in the  
153 neutralization assay. However, more than 90% of individuals remained positive on the Roche  
154 Elecsys anti-nucleocapsid assay for both prior D614G and Beta exposed individuals<sup>33</sup>, despite  
155 low nAb titer level (Extended Data Table 1).

156 Fig. 2a shows the Delta wave participants anti-D614G nAb titers at peak and at BD5. The  $ID_{50}$   
157 geometric mean titer (GMT) was 125 (95% CI 97 – 161) at peak and waned to 85 (95% CI 69 –  
158 104) at BD5, representing an average 1.47 (95% CI 1.32 – 1.67) fold reduction due to waning.  
159 The anti-D614G nAb titers (in log scale) at peak and at BD 5 were highly correlated (Pearson  
160 correlation coefficient 0.89,  $p < 0.0001$ ). Comparing the nAb titers between individuals who were  
161 infected during the Delta wave vs. those who were not infected, we found that the GMTs of  
162 infected individuals was significantly lower than that of uninfected individuals for both anti-  
163 D614G nAb at peak level and at BD5 (Fig. 2b-c). In contrast, we did not find a significant  
164 difference in the degree of antibody loss due to waning ( $\Delta nAb^W$ ) between infected and  
165 uninfected individuals (Fig. 2d).

166 Similarly, for the Omicron wave, we focused on a subgroup of 535 participants from 184  
167 households who had only one prior SARS-CoV-2 infection (vaccinated and repeatedly infected  
168 individuals were removed from the analysis) or remained naïve just before the Omicron wave  
169 (see Table 1 and Extended Data Fig. 2 for a description of participants and Fig. 1 for the timing  
170 of the Omicron wave). Prior SARS-CoV-2 infection was ascertained in a similar fashion as for  
171 the Delta wave (i.e., positivity by anti-nucleocapsid assay and/or rRT-PCR for the first 8 blood  
172 draws). Infections during the Omicron wave were inferred based on the anti-nucleocapsid  
173 antibody level of two pre- and one post- Omicron wave serum samples, as previously described  
174<sup>30</sup>. Two thirds, or 67% (359/535), of participants included in the Omicron BA.1/2 wave analysis

175 were infected by these variants, with attack rates of 77% (149/193) and 61% (210/342) for naïve  
176 and previously infected individuals, respectively.

177 To evaluate nAbs as CoP in the context of Omicron's extensive immune escape, we measured  
178 both the anti-D614G nAb titers and anti-Omicron BA.1 nAb titers for serum samples collected at  
179 blood draw 8 (the blood draw taken shortly before the onset of the Omicron wave, referred to as  
180 BD8 hereafter). Given that none of the participants had been infected by Omicron prior to BD8,  
181 the anti-Omicron BA.1 neutralizing activity at this time point originated from cross-reactive  
182 antibodies elicited by prior variant infections. Thus, the difference between anti-D614G and anti-  
183 BA.1 nAb titers at BD8 represents the quantity of anti-D614G nAbs that failed to recognize  
184 mutated epitopes on Omicron BA.1, resulting in a lack of neutralizing function against Omicron  
185 BA.1. For the remainder of the manuscript, we will use  $\Delta nAb^E$  to represent the quantity of  
186 antibodies able to neutralize D614G but not Omicron BA.1 due to mutations in the Omicron  
187 spike. Similarly to the Delta wave subgroup, a significant proportion of previously infected  
188 individuals in the Omicron wave subgroup exhibited anti-D614G and anti-Omicron nAb titers  
189 below the detection threshold at BD8 (Extended Data Table 1). The absence of detectable nAbs  
190 was also more pronounced when the variant causing prior exposure and the spike used in the  
191 neutralization assay were mismatched. (Extended Data Table 1). Roche Elecsys anti-  
192 nucleocapsid assay remained robust in detecting prior infection <sup>33</sup>, despite low nAb titer level  
193 (Extended Data Table 1).

194 Fig. 2e shows the anti-D614G and the anti-BA.1 nAb titers at BD8 for participants included in  
195 the Omicron wave analysis. The nAb GMT against D614G was 122 (95% CI 103 – 145) and 30  
196 (95% CI 27 – 34) for antibodies that could neutralize BA.1, representing an average 4.01 (95%  
197 CI 3.53 – 4.58) -fold reduction attributed to the immune evasive properties of Omicron. The  
198 anti-D614G and anti-BA.1 nAb titers (in log scale) at BD 8 were modestly correlated (Pearson  
199 correlation coefficient 0.64,  $p < 0.0001$ ). Comparing the nAb titers between individuals who were  
200 infected during the Omicron wave vs. those who were not infected, we did not find significant  
201 differences in GMT levels for anti-D614G nAb, anti-BA.1 nAb, or  $\Delta nAb^E$  (Fig. f-h). However,  
202 it is worth noting that the point estimates of GMTs were higher for uninfected individuals  
203 compared to infected individuals across all three measurements.

204

## 205 **Pre-exposure nAb titer as CoP against variant infection**

206 We conducted mediation analyses in a household transmission modelling framework to  
207 investigate how nAb titers against SARS-CoV-2 variants at the onset of a SARS-CoV-2 wave  
208 mediate the risk of infection during the corresponding epidemic wave. Specifically, following the  
209 causal inference framework proposed by Halloran, et al.<sup>34</sup>, we introduced SARS-CoV-2  
210 transmission probabilities as causal parameters, representing either the risk of acquiring infection  
211 from the general community or the per-contact transmission risk within the household.  
212 Transmission probabilities were dependent on an individual's prior infection history, the level of  
213 pre-existing nAb titers (mediators), and other confounding factors (age, gender, comorbidities).  
214 We fitted a chain-binomial household transmission model, parametrized by the transmission  
215 probabilities, to the infection outcomes of the Delta and Omicron waves among all subgroup  
216 participants and evaluated how the level of nAb titers mediated SARS-CoV-2 transmission  
217 probability. The details of the mediation analysis are described in the Methods Section 3.

218 For the Delta wave mediation analysis, we considered anti-D614G nAb titer at BD5 as  
219 candidate mediator of protection and the quantity of antibodies that had waned from peak  
220 ( $\Delta nAb^W$ ) as putative negative control (i.e., we hypothesize that antibodies lost due to waning  
221 could not conceivably contribute to protection). For the Omicron wave, we considered anti-BA.1  
222 nAb titer at BD8 as candidate mediator of protection and the quantity of nAbs that escape  
223 Omicron neutralization ( $\Delta nAb^E$ ) at BD8 as putative negative control. We used the term “direct  
224 effect” from the causal inference framework to refer to the effect of exposure (prior infection) on  
225 the outcome (repeat infection during the Delta or Omicron wave) absent the mediators (nAb  
226 titers). Conversely, the term “indirect effect” represents the effect of exposure (prior infection)  
227 on the outcome (repeat infection) that operates through the mediators (nAb titers). We estimated  
228 both the direct effect of prior infection and effects mediated through specific nAb titers against  
229 serologically confirmed SARS-CoV-2 infections. We report the estimates of the mediation  
230 analysis for both Delta and Omicron wave in Table 2. For the ease of interpretation, we then  
231 translate the estimated odds ratios into risk reductions ( $1 - \text{odds ratio}$ ), along with other estimates  
232 in causal diagrams depicted in Fig. 3.

233 Our findings indicate that immunity derived from prior infection, overall, reduced the risk of  
234 contracting a Delta wave infection by 61% (95%CI: 59% – 63%) (Fig 3a). Notably, nAbs



235 represented an important mediator of this overall protection: for every 10-fold increase in the  
236 anti-D614G nAb titers at BD5, the risk of infection decreased by 40% (95% CI 19% – 56%). In  
237 contrast, the decline in nAbs from peak levels to BD5 ( $\Delta nAb^W$ ) showed no contribution to the  
238 overall protection, with a risk reduction per 10-fold increase of -1% (95%CI: -21% – 16%). This  
239 result indicated that waning of neutralizing antibodies results in waning of protection, in  
240 agreement with our hypothesis. Furthermore, we estimated that the protection mediated through  
241 anti-D614G nAbs at BD5 accounted for 37% (95% CI: 34% - 40%) of the overall protection  
242 derived from prior infection, suggesting that over half of the protection against Delta was not  
243 mediated by serum nAbs against D614G. Lastly, our analysis indicated that individuals  
244 reinfected with the Delta variant were 78% (95% CI: 24% – 94%) less likely to transmit the  
245 infection to other household members compared to those who experienced primary infections  
246 (Fig. 3a). This finding suggested that even in cases where prior immunity is not sufficient to  
247 block reinfection with the Delta variant, infection-induced immunity still offered sizable  
248 mitigation against onward transmission.

249 The causal diagram depicting the mediation analysis for the Omicron wave is illustrated in  
250 Fig. 3b. Our findings indicate that, overall, prior infection-derived immunity resulted in a 37%  
251 (95%CI: 35% – 38%) reduction in the risk of contracting an Omicron wave infection, a notably  
252 lower effect compared to that of the Delta wave. We observed that, anti-Omicron nAbs at BD8  
253 significantly mediated protection against the Omicron BA.1/2 variants: for every 10-fold  
254 increase in anti-Omicron nAb titers, the risk of Omicron BA.1/2 infection decreased by 28%  
255 (95% CI: 6% – 44%). Conversely, antibodies unable to neutralize Omicron due to immune  
256 escape ( $\Delta nAb^E$ ) did not mediate protection against Omicron BA.1/2 infection, with risk  
257 reduction of -1% (95% CI: -21% – 16%) per 10-fold titer increase. Furthermore, we estimated  
258 that the protection mediated through anti-BA.1 nAbs at BD8 accounted for only 11% (95% CI:  
259 9% - 12%) of the total protection conferred by prior exposure. This, coupled with the observation  
260 that Omicron BA.1 caused an average of 4.01-fold drop in nAb titers (Fig. 2e), underscores  
261 Omicron BA.1/2's ability to evade host protective immunity mediated through nAbs.  
262 Additionally, in contrast to the Delta wave, individuals reinfected with the Omicron variant were  
263 as likely to transmit the infection to other household members compared to those who  
264 experienced primary infections (risk reduction: -17%, (95% CI: -110% – 35%)). These

265 observations suggested that Omicron not only evaded prior immunity's protection against  
266 acquisition of infection but also escaped protection against onward transmission.

267 Although neutralizing titers measured at BD5 and BD8 offered a temporally proximate  
268 evaluation of protective immunity preceding the onset of the Delta and Omicron waves, we  
269 could not identify the immune mediators responsible for the direct effects of prior immunity (i.e.,  
270 the fraction of protection that was not mediated by nAbs) due to lack of additional serum  
271 biomarkers. We could however estimate the potential for these direct effects to wane over time.  
272 To do so, we modeled an exponential decline for the direct effect based on the time elapsed since  
273 prior infection and jointly estimated the duration of protection for both the Delta and Omicron  
274 waves' analysis. We found that protection not mediated by nAbs decreased with time, with a  
275 waning half-life of 121 (95%CI: 72 – 242) days (Fig. 3, Table 2). After adjusting for waning, the  
276 effect sizes of protection from direct effects were similar for both variants, with odds ratios of  
277 acquiring infection (compared to naïve individuals) of 0.34 (95% CI: 0.17, 0.68) and 0.29 (95%  
278 CI: 0.17, 0.50) for the Delta and Omicron wave, respectively, in the absence of waning (Table 2).  
279 These results suggested that, while Omicron escaped pre-existing neutralizing antibodies,  
280 protection from other immune effectors was preserved against this variant. The waning half-life  
281 of protection not mediated by nAbs was estimated at approximately 4 months in our study,  
282 comparable to the reported waning timescale of T-cell immunity<sup>35,36</sup>. Several sensitivity  
283 analyses demonstrating the robustness of the findings of the mediation analysis were reported in  
284 the Methods Section 3.2 – 3.4.

285

286

## 287 **Discussion**

288 In this cohort of unvaccinated individuals, we found that nAb titers immediately before the onset  
289 of the Delta wave (i.e., anti-D614G nAb level at BD5) correlated with protection against Delta  
290 wave infections. Moreover, we demonstrated that nAb titers lost over time due to waning (i.e.,  
291  $\Delta nAb^W$ ) were not associated with protection, aligning with the expectation that waning of nAbs  
292 in serum corresponds to waning of clinical protection. For the Omicron wave subgroup, we  
293 further investigated the impact of immune escape against protection mediated through nAbs. We  
294 found that only anti-Omicron BA.1 nAbs correlated with protection against infection during the

295 Omicron BA.1/2 wave, whereas anti-D614G nAbs that were unable to neutralize Omicron BA.1  
296 due to spike escape mutations did not protect. This indicated that antibodies capable of  
297 neutralizing D614G but not Omicron BA.1 *in vitro* translates to a diminished protection against  
298 Omicron BA.1/2 infection among PHIRST-C participants. The identification of variant-  
299 neutralizing antibodies derived from infection-induced immunity as CoPs against infections for  
300 both Delta and Omicron variants aligns with findings from studies on variant-specific correlates  
301 for vaccine-induced or hybrid immunity<sup>21-24</sup>. Considering that antibody-mediated protection  
302 against acquisition of infection likely operates at the mucosal site rather than in serum, it is  
303 interesting that serum antibodies levels can anticipate protection<sup>26</sup>. In a recent analysis of the  
304 data from the COVE trial, Zhang et. al. further demonstrated that boosting of nAb titers against  
305 Omicron by a third dose of mRNA-1273 vaccine, afforded additional protection against Omicron  
306 compared to individuals who only received 2 doses of the mRNA-1273 vaccine.<sup>22</sup> Collectively,  
307 these empirical data lend support for using nAbs against circulating variant as immuno-bridging  
308 markers for periodic vaccine updates.

309 While a comprehensive understanding of the role of nAbs in SARS-CoV-2 protection is  
310 important, a key finding of our study is that nAb titers did not fully mediate protection conferred  
311 by prior infection. In the case of the Delta wave subgroup, we estimate that anti-D614G nAbs  
312 mediate 37% of protection, a proportion comparable to vaccine-induced nAbs<sup>15</sup>. In contrast, for  
313 the Omicron BA.1/2 wave subgroup, anti-Omicron BA.1 nAbs are estimated to mediate only 11%  
314 of protection, which was substantially lower than that observed for the Delta wave. This low  
315 percentage of protection mediated by nAbs for the Omicron BA.1/2 wave could be attributed to  
316 the highly immune evasive nature of Omicron against neutralizing activity. Omicron effectively  
317 rendered a significant proportion of serum anti-D614G nAbs nonfunctional against Omicron.  
318 The large proportion of overall protection that was not mediated by nAbs could be explained by  
319 a variety of immune mechanisms, including the Fc-effector function of binding antibodies, and  
320 T-cell functions, both of which are resilient against mutations in VOCs<sup>14,37</sup>. Additionally,  
321 SARS-CoV-2 initially infects and predominantly transmits through the upper respiratory tract.  
322 Mucosal immunity in the upper respiratory tract therefore likely plays a key role in preventing  
323 SARS-CoV-2 infection, and may not be fully represented by immune markers in serum<sup>38</sup>. Our  
324 study validates the use of serum nAbs as CoP against reinfection but also suggests potential  
325 important roles for other candidate functions that could act as “co-correlates” of protection<sup>39</sup>.

326 This is particularly important because these mechanisms may be more broadly cross-protective  
327 against future variants than neutralizing antibodies. Future CoP analyses incorporating  
328 measurements of T-cell immunity and non-neutralizing antibody functions, ideally at the mucosal  
329 site, could potentially disentangle these important protective mechanisms and inform design of  
330 next generation vaccines<sup>26,40-42</sup>.

331 Our study has several limitations. Firstly, the vaccination rate in the PHIRST-C cohort was  
332 low at the time of the analysis; with <20% participants fully vaccinated prior to the Omicron  
333 BA.1/2 wave (thus excluded from our analysis). Consequently, we lacked sufficient statistical  
334 power to assess CoPs for vaccine-induced (or hybrid) immunity and compare with our findings  
335 for infection-induced immunity in the same cohort. Secondly, we focused on SARS-CoV-2  
336 infections that were ascertained by seroconversion or amnestic boosting of the anti-nucleocapsid  
337 antibodies. However, not all PCR-positive SARS-CoV-2 infections led to systemic antibody  
338 response<sup>30,43,44</sup>. Thus, our CoP analysis does not account for protection against abortive or  
339 transient infections that do not lead to systemic antibody responses. We also could not evaluate  
340 CoPs against symptomatic cases, as there was no systemic monitoring of SARS-CoV-2  
341 symptoms for the cohort population during the Omicron BA.1/2 wave. Further, severe outcomes  
342 (hospitalizations and deaths) due to SARS-CoV-2 infections were rare throughout the course of  
343 the PHIRST-C study and evaluation of protection against those outcomes is under-powered.  
344 Understanding protection against severe outcomes is important from both clinical and public  
345 health perspective, thus warranting further studies. Thirdly, the strains of antigens used in  
346 neutralization assay were not perfectly matched to the circulating variants in the CoP analysis.  
347 For the Delta wave analysis, we evaluated anti-D614G antibody titers (rather than anti-Delta  
348 titers). Although Delta is not as immune evasive as Omicron with respect to D614G, there are  
349 substitutions on the spike of Delta (i.e., L452R, T478K) that are linked to moderate antigenic  
350 escape<sup>45,46</sup>. In addition, though infections were predominantly caused by the Delta variant  
351 during the Delta wave epidemic, other variants also circulated at low levels during the same time  
352 period, including Alpha and C.1.2<sup>30</sup>. Similarly, genomic surveillance revealed that while  
353 Omicron BA.1 accounted for the majority of infections during the Omicron wave, Omicron BA.2  
354 also co-circulated, with potential antigenic spike substitutions (e.g., T376A, D405N, R408S) that  
355 were not present in BA.1<sup>30,46,47</sup>. Thus, using a BA.1-specific neutralizing assay may introduce  
356 bias in our CoP analysis, particularly against Omicron BA.2. Lastly, we only measured serum

357 antibodies, but did not have any information on antibody response at the mucosal site or on cell-  
358 mediated immunity. While serum IgG nAbs may transudate into the nasal mucosa and thereby  
359 play a role in protection, the contribution of locally produced nasal IgA nAb remains to be  
360 investigated.

361 Moving forward, future works focusing on understanding how protective immunity  
362 accumulates through repeated infections, vaccinations, and hybrid immunity, and identifying a  
363 suite of predictive markers of protection reflecting different arms of immune responses, are key  
364 to anticipating long-term SARS-CoV-2 burden, optimizing vaccine boosters, and designing next  
365 generation SARS-CoV-2 vaccines.

366

## 367 **Acknowledgment**

368 The findings and conclusions in this report are those of the authors and do not necessarily  
369 represent the official position of the NIH or the U.S. Centers for Disease Control and Prevention.

370 **Funding:** This work was supported by the National Institute for Communicable Diseases of the  
371 National Health Laboratory Service and the U.S. Centers for Disease Control and Prevention  
372 [cooperative agreement number: 6 U01IP001048] and Wellcome Trust (grant number  
373 221003/Z/20/Z) in collaboration with the Foreign, Commonwealth and Development Office,  
374 United Kingdom. PLM and JNB are supported by the Bill and Melinda Gates Foundation  
375 through the Global Immunology and Immune Sequencing for Epidemic Response (GIISER)  
376 program (INV-030570) and receive funding from the Wellcome Trust (226137/Z/22/Z). PLM is  
377 supported by the South African Research Chairs Initiative of the Department of Science and  
378 Innovation and National Research Foundation of South Africa and the SA Medical Research  
379 Council SHIP program.

## 380 **Author Contributions Statement**

381 KS, JNB, ST, JK, AvG, MLM, NW, JM, NAM, KK, LL, CV, PLM, CC designed the experiments.  
382 JNB, CC, JK, PLM and ST accessed and verified the underlying data. JNB, ST, JK, VSM, QM,  
383 HK, AvG, MLM, NW, JM, MC, NAM, KK, LL, JdT, TM, PLM, CC collected the data and  
384 performed laboratory experiments. KS, JNB, ST, JK, AvG, MLM, NW, JM, MC, NAM, KK, LL,

385 JdT, TM, CV, and CC analyzed the data and interpreted the results. KS, JNB, CV, PLM, and CC  
386 drafted the manuscript. All authors critically reviewed the article. All authors had access to all  
387 the data reported in the study.

### 388 **Competing Interests Statement**

389 CC has received grant support from Sanofi Pasteur, US CDC, the Bill & Melinda Gates  
390 Foundation, the Taskforce for Global Health, Wellcome Trust and the South African Medical  
391 Research Council. AvG has received grant support from Sanofi Pasteur, Pfizer related to  
392 pneumococcal vaccine, CDC and the Bill & Melinda Gates Foundation. NW reports grants from  
393 Sanofi Pasteur and the Bill & Melinda Gates Foundation. NAM has received a grant to his  
394 institution from Pfizer to conduct research in patients with pneumonia and from Roche to collect  
395 specimens to assess a novel TB assay. JM has received grant support from Sanofi Pasteur. The  
396 remaining authors declare no competing interests

### 397 **Consortia Authorship**

398 The PHIRST-C group: Jinal N. Bhiman<sup>2,3</sup>, Amelia Buys<sup>4</sup>, Maimuna Carrim<sup>4,7</sup>, Cheryl Cohen<sup>4,5</sup>,  
399 Linda de Gouveia<sup>4</sup>, Mignon du Plessis<sup>4,7</sup>, Jacques du Toit<sup>11</sup>, Francesc Xavier Gómez-Olivé<sup>11</sup>,  
400 Kathleen Kahn<sup>11</sup>, Kgaugelo Patricia Kgasago<sup>9</sup>, Jackie Kleynhans<sup>4,5</sup>, Retshidisitswe Kotane<sup>4</sup>,  
401 Limakatso Lebina<sup>9</sup>, Neil A Martinson<sup>9,10</sup>, Meredith L McMorrow<sup>6,8</sup>, Tumelo Moloantoa<sup>4</sup>, Jocelyn  
402 Moyes<sup>4,5</sup>, Stefano Tempia<sup>4,5,6</sup>, Stephen Tollman<sup>11</sup>, Anne von Gottberg<sup>4,7</sup>, Floidy Wafawanaka<sup>11</sup>,  
403 Nicole Wolter<sup>4,7</sup>

404

405 **Tables:**

406 **Table 1: Characteristics of the PHIRST-C cohort's Delta wave subgroup and Omicron wave subgroup**  
 407 **populations, respectively.** \*PLWH: people living with HIV. \*\*Here it indicates if a participant of the Delta/Omicron  
 408 wave subgroup was infected (either primary or repeat infection) during the Delta/Omicron BA.1 wave.

	<b>Delta wave subgroup</b> <b>196 households</b>	<b>Omicron wave subgroup</b> <b>184 households</b>
<b>Characteristics</b>	Number of individuals (%)	Number of individuals (%)
All	797 (100)	535 (100)
<b>Study site</b>		
Rural	427 (54)	300 (56)
Urban	370 (46)	235 (44)
<b>Age group, in years</b>		
0-4	90 (11)	77 (14)
5-12	270 (34)	231 (43)
13-18	111 (14)	80 (15)
19-34	126 (16)	84 (16)
35-59	126 (16)	43 (8)
60+	74 (9)	20 (4)
<b>Sex</b>		
Male	324 (41)	229 (43)
Female	473 (59)	306 (57)
<b>Household size</b>		
3-5	372 (47)	254 (48)
6-8	264 (33)	197 (37)
9-12	124 (15)	72 (13)
13+	37 (5)	12 (2)
<b>HIV status</b>		
Negative	673 (85)	496 (93)
PLWH*	97 (12)	31 (6)
Unknown	27 (3)	8 (1)
<b>Prior immunity</b>		
Naive	544 (68)	193 (36)
Previously infected	253 (32)	342 (64)
Variant of prior infection:		
D614G	113 (14)	61 (11)
Beta	140 (18)	120 (22)
Delta	–	161 (31)
<b>Infected**</b>		
Yes	273 (34)	359 (67)
No	524 (66)	176 (33)

409 **Table 2: Mediation analysis for nAbs as CoPs against Delta and Omicron wave infections, with a waning**  
 410 **model for direct effect.** Average and 95% CIs are provided for each of the model parameters.  $\Delta nAb^W$ : the quantity  
 411 of anti-D614G nAbs waned from peak level to that at BD5.  $\Delta nAb^E$ : the quantity of antibodies that can neutralize  
 412 D614G but fail to neutralize Omicron BA.1 at BD8 due to Omicron’s immune escape.

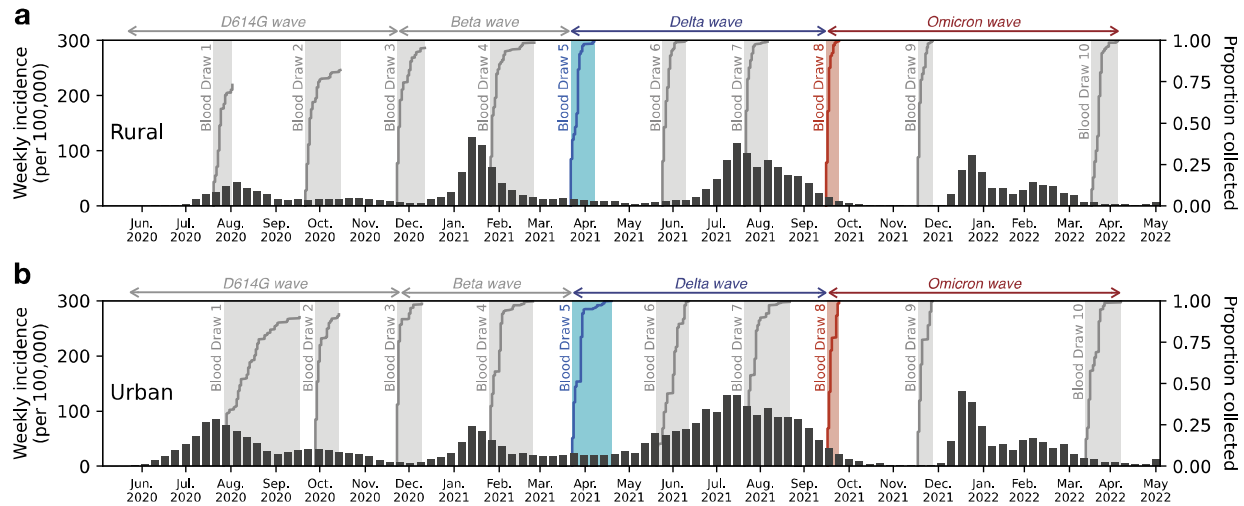
Wave		Delta	Omicron	
<b>Protection against reinfection</b>	<b>Direct effect</b> (Protection absent of nAbs)	<b>Effect size</b> (odds ratio, absent of waning)	0.34 (0.17, 0.68)	0.29 (0.17, 0.50)
		<b>Waning half-life</b> (days)	121 (72, 242)	
	<b>Mediators effect</b> (Protection from nAbs)	<b>Anti-D614G nAb</b> (odds ratio, per 10-fold increase)	0.60 (0.44, 0.81)	–
		$\Delta nAb^W$ (odds ratio, per 10-fold increase)	1.01 (0.74, 1.37)	–
		<b>Anti-Omicron BA.1 nAb</b> (odds ratio, per 10-fold increase)	–	0.72 (0.56, 0.94)
		$\Delta nAb^E$ (odds ratio, per 10-fold increase)	–	1.01 (0.84, 1.21)
	<b>Total protection</b> (relative risk compared to naïve individuals)		0.39 (0.37, 0.41)	0.63 (0.62, 0.65)
	<b>Proportion of protection mediated by nAbs</b>		37% (34%, 40%)	11% (9%, 12%)
	<b>Protection against onward transmission</b> (Odds ratio compared to naïve individuals)		0.22 (0.06, 0.76)	1.17 (0.65, 2.10)

413

414



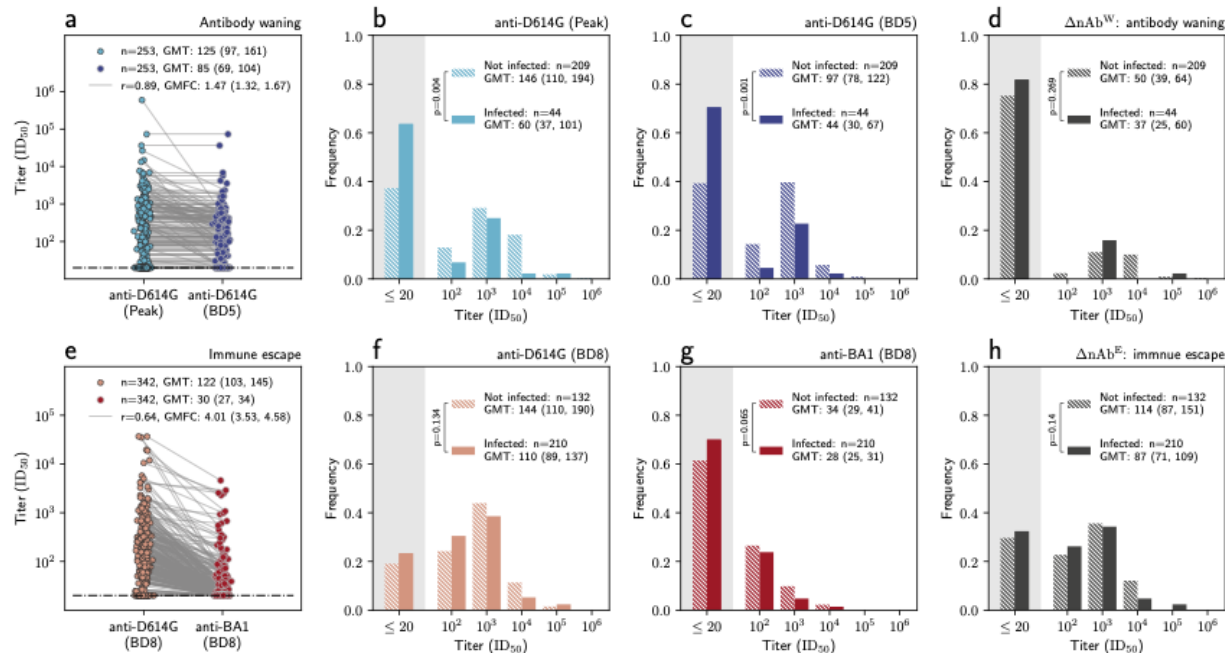
415 **Figures:**



416

417 **Fig. 1: Timing of cohort sample collections with respect to SARS-CoV-2 variants' circulations in the two study**  
418 **sites. a,** Timing of the blood draws with respect to the SARS-CoV-2 epidemic waves in the rural site (Agincourt) of  
419 the PHIRST-C cohort. Bar plot represents the weekly incidence (per 100,000 population) of SARS-CoV-2 cases  
420 from routine surveillance data collected in Ehlanzeni District, Mpumalanga Province (where rural participants  
421 reside). The shaded areas represent the timing of the serum sample collections for the 10 blood draws. Each curve  
422 within the shaded area indicates the cumulative proportion of participants' serum samples collected over time. The  
423 Delta wave subgroup analysis focuses on nAb titers among serum samples collected during blood draw 5 (blue  
424 shade); the Omicron BA.1 wave analysis focuses on nAb titers among serum samples collected during blood draw 8  
425 (red shade). **b,** Same as (A), but for the urban site (Klerksdorp). The routine surveillance data (bar plot) were  
426 collected from Dr. Kenneth Kaunda District, North West Province (where urban participants reside).

427



428

429

430

431

432

433

434

435

436

437

438

439

440

441

442

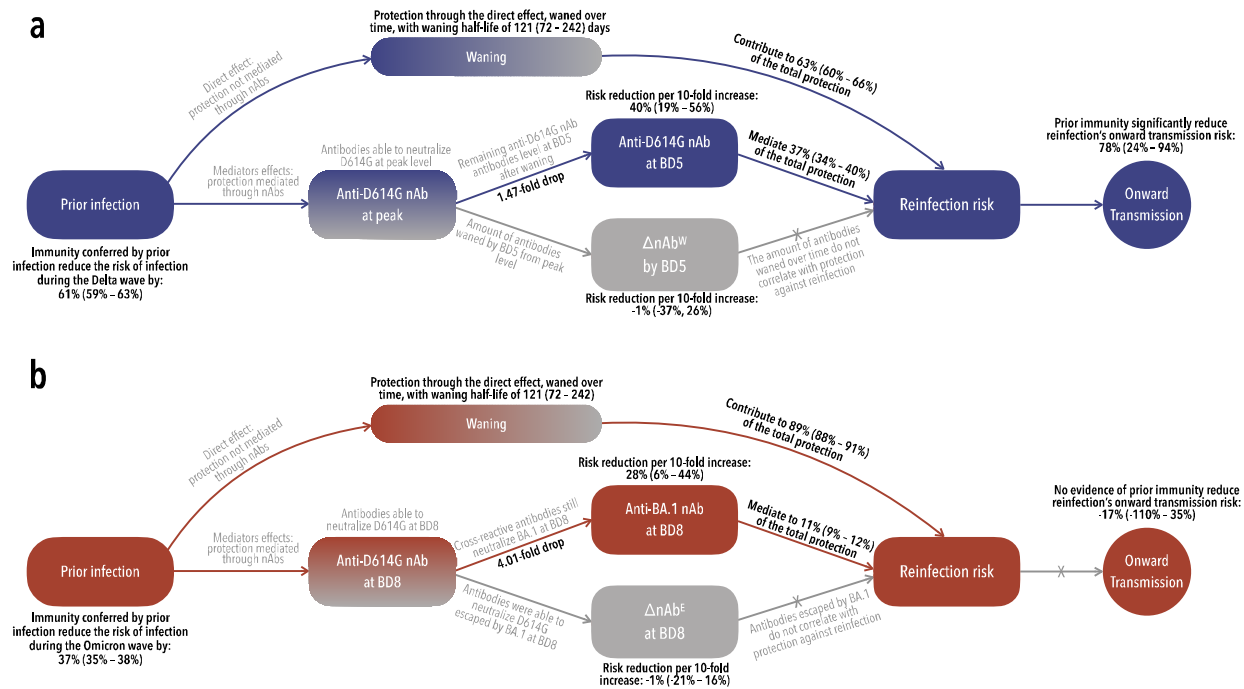
443

444

445

446

**Fig. 2: Anti-D614G and anti-BA.1 nAb titers for the Delta wave and the Omicron wave analysis.** **a**, for Delta wave subgroup, the distribution of the peak anti-D614G nAb titer up to BD5 (light blue dots) and the anti-D614G nAb titer at BD5 (dark blue dots), among individuals who had one prior SARS-CoV-2 infection before blood draw 5. Each dot represents one individual, with two measurements of the same individual connected through a gray line. GMFC: geometric fold change from peak anti-D614G titer to that at BD5; GMT: geometric mean titer; r: Pearson correlation coefficient. **b**, for Delta wave subgroup, the distribution of the peak anti-D614G nAb titer up to BD5, stratified by individuals who were infected during the Delta wave (solid bar) vs those who were not infected (dashed bar). Independent samples t-test (two-sided) is used to determine the statistical significance (p-value reported on the legend) of difference between the GMT of the two groups. **c**, same as **b** but for anti-D614G nAb titers at BD5. **d**, same as **b** but for  $\Delta nAb^W$  (defined as the difference between anti-D614G titers at peak and at BD5). **e**, for Omicron wave subgroup, the distribution of anti-D614G nAb titers (light red dots) and anti-BA.1 titers at BD8 (dark red dots), among individuals who had one prior SARS-CoV-2 infection before BD8. Each dot represents one individual, with two measurements of the same individual connected through a gray line. **f**, for the Omicron wave subgroup, the distribution of the anti-D614G nAb titer at BD5, stratified by individuals who were infected during the Omicron wave (solid bar) vs those who were not infected (dashed bar). Independent samples t-test (two-sided) is used to determine the statistical significance (p-value reported on the legend) of difference between the GMT of the two groups. **g**, same as **f** but for anti-BA.1 nAb titers at BD8. **h**, same as **f** but for  $\Delta nAb^E$  (defined as the difference between anti-BA.1 and anti-D614G titers at BD8).



447

448 **Figure 3: Causal diagrams for the mediation analyses. a:** Causal diagram of the Delta wave mediation analysis  
 449 showing the hypothesized relationship between prior immunity (induced by prior SARS-CoV-2 infection) and  
 450 SARS-CoV-2 infection (outcome of interest) during Delta wave. The mediators of interest are anit-D614G nAbs at  
 451 BD5 and  $\Delta nAb^W$  (the quantity of anti-D614G nAbs waned from peak level to that at BD5). The direct effect  
 452 represents protection operating through immune mechanisms other than the mediators of interest. We hypothesize  
 453 that the direct effect could wane over time since the initial immune exposure. For the prospective cohort data, both  
 454 mediator-outcome confounding and exposure-outcome confounding factors need to be adjusted for in the mediation  
 455 analysis, as the immune exposure (prior SARS-CoV-2 infection) was not randomly assigned (unlike SARS-CoV-2  
 456 randomized-control vaccine trials where vaccination was randomly assigned to the participants). Furthermore,  
 457 cohort participants may experience heterogenous levels of SARS-CoV-2 exposure due to different intensity SARS-  
 458 CoV-2 transmission in their household settings. We adjust this by embedding the mediation analysis in a mechanistic  
 459 household transmission model (detailed in Methods Section 3). We also look at the impact of prior immunity on the  
 460 reduction of onward transmission, conditional on the failure of preventing reinfection. The estimates of the Delta  
 461 wave mediation analysis are presented in Table 2. **b:** Same as a but for the Omicron wave analysis. The mediators of  
 462 interest are anit-BA.1 nAbs at BD8 and  $\Delta nAb^E$  (the quantity of antibodies that can neutralize D614G but fail to  
 463 neutralize Omicron BA.1 at BD8 due to Omicron's immune escape.). The estimates of the Omicron wave mediation  
 464 analysis are presented in Table 2.

465

466

467 **Reference:**

- 468 1. Statement on the fifteenth meeting of the IHR (2005) Emergency Committee on the  
469 COVID-19 pandemic. [https://www.who.int/news/item/05-05-2023-statement-on-the-](https://www.who.int/news/item/05-05-2023-statement-on-the-fifteenth-meeting-of-the-international-health-regulations-(2005)-emergency-committee-regarding-the-coronavirus-disease-(covid-19)-pandemic)  
470 [fifteenth-meeting-of-the-international-health-regulations-\(2005\)-emergency-committee-](https://www.who.int/news/item/05-05-2023-statement-on-the-fifteenth-meeting-of-the-international-health-regulations-(2005)-emergency-committee-regarding-the-coronavirus-disease-(covid-19)-pandemic)  
471 [regarding-the-coronavirus-disease-\(covid-19\)-pandemic.](https://www.who.int/news/item/05-05-2023-statement-on-the-fifteenth-meeting-of-the-international-health-regulations-(2005)-emergency-committee-regarding-the-coronavirus-disease-(covid-19)-pandemic)
- 472 2. WHO Coronavirus (COVID-19) Dashboard. <https://covid19.who.int/>.
- 473 3. WHO – COVID19 Vaccine Tracker. <https://covid19.trackvaccines.org/agency/who/>.
- 474 4. Watson, O. J. *et al.* Global impact of the first year of COVID-19 vaccination: a  
475 mathematical modelling study. *Lancet Infect. Dis.* **22**, 1293–1302 (2022).
- 476 5. Gozzi, N. *et al.* Estimating the impact of COVID-19 vaccine inequities: a modeling study.  
477 *Nat. Commun.* **14**, 3272 (2023).
- 478 6. Wang, Q. *et al.* Mapping global acceptance and uptake of COVID-19 vaccination: A  
479 systematic review and meta-analysis. *Commun. Med.* **2**, 113 (2022).
- 480 7. Lazarus, J. V. *et al.* A survey of COVID-19 vaccine acceptance across 23 countries in 2022.  
481 *Nat. Med.* **29**, 366–375 (2023).
- 482 8. Bergeri, I. *et al.* Global SARS-CoV-2 seroprevalence from January 2020 to April 2022: A  
483 systematic review and meta-analysis of standardized population-based studies. *PLoS Med.*  
484 **19**, e1004107 (2022).
- 485 9. Lewis, H. C. *et al.* SARS-CoV-2 infection in Africa: a systematic review and meta-analysis  
486 of standardised seroprevalence studies, from January 2020 to December 2021. *BMJ Glob*  
487 *Health* **7**, (2022).
- 488 10. Wang, Q. *et al.* Antibody evasion by SARS-CoV-2 Omicron subvariants BA.2.12.1, BA.4  
489 and BA.5. *Nature* **608**, 603–608 (2022).

- 490 11. Ito, J. *et al.* Convergent evolution of SARS-CoV-2 Omicron subvariants leading to the  
491 emergence of BQ.1.1 variant. *Nat. Commun.* **14**, 2671 (2023).
- 492 12. Cao, Y. *et al.* BA.2.12.1, BA.4 and BA.5 escape antibodies elicited by Omicron infection.  
493 *Nature* **608**, 593–602 (2022).
- 494 13. Cao, Y. *et al.* Imprinted SARS-CoV-2 humoral immunity induces convergent Omicron RBD  
495 evolution. *Nature* **614**, 521–529 (2023).
- 496 14. Goldblatt, D., Alter, G., Crotty, S. & Plotkin, S. A. Correlates of protection against SARS-  
497 CoV-2 infection and COVID-19 disease. *Immunol. Rev.* **310**, 6–26 (2022).
- 498 15. Gilbert, P. B. *et al.* Immune correlates analysis of the mRNA-1273 COVID-19 vaccine  
499 efficacy clinical trial. *Science* **375**, 43–50 (2022).
- 500 16. Fong, Y. *et al.* Immune correlates analysis of the PREVENT-19 COVID-19 vaccine efficacy  
501 clinical trial. *Nat. Commun.* **14**, 331 (2023).
- 502 17. Fong, Y. *et al.* Immune correlates analysis of the ENSEMBLE single Ad26.COV2.S dose  
503 vaccine efficacy clinical trial. *Nat Microbiol* **7**, 1996–2010 (2022).
- 504 18. Feng, S. *et al.* Correlates of protection against symptomatic and asymptomatic SARS-CoV-  
505 2 infection. *Nat. Med.* **27**, 2032–2040 (2021).
- 506 19. Khoury, D. S. *et al.* Neutralizing antibody levels are highly predictive of immune protection  
507 from symptomatic SARS-CoV-2 infection. *Nat. Med.* **27**, 1205–1211 (2021).
- 508 20. Earle, K. A. *et al.* Evidence for antibody as a protective correlate for COVID-19 vaccines.  
509 *Vaccine* **39**, 4423–4428 (2021).
- 510 21. Atti, A. *et al.* Antibody correlates of protection against Delta infection after vaccination: A  
511 nested case-control within the UK-based SIREN study. *J. Infect.* **87**, 420–427 (2023).

- 512 22. Zhang, B. *et al.* Omicron COVID-19 immune correlates analysis of a third dose of mRNA-  
513 1273 in the COVE trial. *bioRxiv* (2023) doi:10.1101/2023.10.15.23295628.
- 514 23. Hertz, T. *et al.* Correlates of protection for booster doses of the SARS-CoV-2 vaccine  
515 BNT162b2. *Nat. Commun.* **14**, 4575 (2023).
- 516 24. Gilboa, M. *et al.* Factors Associated With Protection From SARS-CoV-2 Omicron Variant  
517 Infection and Disease Among Vaccinated Health Care Workers in Israel. *JAMA Netw Open*  
518 **6**, e2314757 (2023).
- 519 25. Tang, J. *et al.* Respiratory mucosal immunity against SARS-CoV-2 after mRNA vaccination.  
520 *Sci Immunol* **7**, eadd4853 (2022).
- 521 26. Knisely, J. M. *et al.* Mucosal vaccines for SARS-CoV-2: scientific gaps and opportunities-  
522 workshop report. *NPJ Vaccines* **8**, 53 (2023).
- 523 27. Miyamoto, S. *et al.* Infectious virus shedding duration reflects secretory IgA antibody  
524 response latency after SARS-CoV-2 infection. *Proc. Natl. Acad. Sci. U. S. A.* **120**,  
525 e2314808120 (2023).
- 526 28. Markov, P. V. *et al.* The evolution of SARS-CoV-2. *Nat. Rev. Microbiol.* **21**, 361–379 (2023).
- 527 29. Cohen, C. *et al.* SARS-CoV-2 incidence, transmission, and reinfection in a rural and an  
528 urban setting: results of the PHIRST-C cohort study, South Africa, 2020-21. *Lancet Infect.*  
529 *Dis.* (2022) doi:10.1016/S1473-3099(22)00069-X.
- 530 30. Sun, K. *et al.* Rapidly shifting immunologic landscape and severity of SARS-CoV-2 in the  
531 Omicron era in South Africa. *Nat. Commun.* **14**, 246 (2023).
- 532 31. Pulliam, J. R. C. *et al.* Increased risk of SARS-CoV-2 reinfection associated with emergence  
533 of Omicron in South Africa. *Science* eabn4947 (2022).

- 534 32. Sun, K. *et al.* SARS-CoV-2 transmission, persistence of immunity, and estimates of  
535 Omicron's impact in South African population cohorts. *Sci. Transl. Med.* eabo7081 (2022).
- 536 33. Elecsys® Anti-SARS-CoV-2. *Diagnostics*  
537 <https://diagnostics.roche.com/us/en/products/params/elecsys-anti-sars-cov-2.html>.
- 538 34. Halloran, M. E. & Struchiner, C. J. Causal inference in infectious diseases. *Epidemiology* **6**,  
539 142–151 (1995).
- 540 35. Cohen, K. W. *et al.* Longitudinal analysis shows durable and broad immune memory after  
541 SARS-CoV-2 infection with persisting antibody responses and memory B and T cells. *Cell*  
542 *Rep Med* **2**, 100354 (2021).
- 543 36. Dan, J. M. *et al.* Immunological memory to SARS-CoV-2 assessed for up to 8 months after  
544 infection. *Science* **371**, (2021).
- 545 37. Eser, T. M. *et al.* Nucleocapsid-specific T cell responses associate with control of SARS-  
546 CoV-2 in the upper airways before seroconversion. *Nat. Commun.* **14**, 2952 (2023).
- 547 38. Havervall, S. *et al.* Anti-Spike Mucosal IgA Protection against SARS-CoV-2 Omicron  
548 Infection. *N. Engl. J. Med.* **387**, 1333–1336 (2022).
- 549 39. Plotkin, S. A. Vaccines: correlates of vaccine-induced immunity. *Clin. Infect. Dis.* **47**, 401–  
550 409 (2008).
- 551 40. Morens, D. M., Taubenberger, J. K. & Fauci, A. S. Rethinking next-generation vaccines for  
552 coronaviruses, influenzaviruses, and other respiratory viruses. *Cell Host Microbe* **31**, 146–  
553 157 (2023).
- 554 41. Topol, E. J. & Iwasaki, A. Operation Nasal Vaccine-Lightning speed to counter COVID-19.  
555 *Science immunology* vol. 7 eadd9947 (2022).

- 556 42. Fact Sheet: HHS Details \$5 Billion ‘Project NextGen’ Initiative to Stay Ahead of COVID-  
557 19. <https://aspr.hhs.gov/newsroom/Pages/ProjectNextGen-May2023.aspx>.
- 558 43. Liu, W. *et al.* Predictors of Nonseroconversion after SARS-CoV-2 Infection. *Emerg. Infect.*  
559 *Dis.* **27**, 2454–2458 (2021).
- 560 44. Lindeboom, R. G. H. *et al.* Human SARS-CoV-2 challenge resolves local and systemic  
561 response dynamics. *medRxiv* (2023) doi:10.1101/2023.04.13.23288227.
- 562 45. McCallum, M. *et al.* Molecular basis of immune evasion by the Delta and Kappa SARS-  
563 CoV-2 variants. *Science* **374**, 1621–1626 (2021).
- 564 46. Wilks, S. H. *et al.* Mapping SARS-CoV-2 antigenic relationships and serological responses.  
565 *Science* **382**, eadj0070 (2023).
- 566 47. Tegally, H. *et al.* Emergence of SARS-CoV-2 Omicron lineages BA.4 and BA.5 in South  
567 Africa. *Nat. Med.* (2022) doi:10.1038/s41591-022-01911-2.
- 568 48. Wibmer, C. K. *et al.* SARS-CoV-2 501Y.V2 escapes neutralization by South African  
569 COVID-19 donor plasma. *Nat. Med.* (2021) doi:10.1038/s41591-021-01285-x.
- 570 49. Netzl, A. *et al.* Analysis of SARS-CoV-2 Omicron Neutralization Data up to 2022-01-28.  
571 *bioRxiv* 2021.12.31.474032 (2023) doi:10.1101/2021.12.31.474032.  
572  
573



## 574 **Methods**

575 **Ethics statement:** The PHIRST-C protocol was approved by the University of Witwatersrand  
576 Human Research Ethics Committee (Reference 150808) and the U.S. Centers for Disease  
577 Control and Prevention's Institutional Review Board relied on the local review (#6840). The  
578 protocol was registered on [clinicaltrials.gov](https://clinicaltrials.gov) on 6 August 2015 and updated on 30 December  
579 2020 (<https://clinicaltrials.gov/ct2/show/NCT02519803>). Participants receive grocery store  
580 vouchers of ZAR50 (USD 3) per visit to compensate for time required for specimen collection  
581 and interview. All participants provided informed consent for study participation. For minors,  
582 consent was obtained from the parent or guardian.

### 583 **1. Inferring Delta and Omicron wave infections based on longitudinal serum samples.**

584 We have previously described the serologic inference method for SARS-CoV-2 infections among  
585 the PHIRST-C cohort participants during the Delta wave (3<sup>rd</sup> SARS-CoV-2 wave) and the  
586 Omicron wave (4<sup>th</sup> SARS-CoV-2 wave)<sup>30</sup>. To briefly summarize, ascertainment of Delta wave  
587 infections was based on the serial serologic readout of blood draws 5 and 6 (both before the  
588 Delta wave, figure 1A-B), and 8 (post Delta wave), measured by the Roche Elecsys Anti-SARS-  
589 CoV-2 nucleocapsid assay<sup>33</sup>. The participants' serologic trajectories were then grouped into 13  
590 categories of distinct serum antibody patterns, reflecting the rise, waning, and/or amnestic  
591 boosting of anti-nucleocapsid antibody levels. Because the Delta wave was also covered by  
592 intense virologic sampling with twice-weekly nasopharyngeal swab collection, we grouped the  
593 13 serologic categories into indicators of either presence or absence of SARS-CoV-2 infection to  
594 achieve the highest concordance with rRT-PCR-confirmed Delta infections. The Omicron wave  
595 was not covered by the intense PCR testing; however, the timing of blood draws 8, 9, and 10  
596 with respect to the Omicron wave is similar to that of blood draws 5, 6, and 8 with respect to the  
597 Delta wave (figure 1A-B). We thus apply the same classification method of serial serologic  
598 trajectories defined by blood draws 8, 9, and 10 to infer SARS-CoV-2 infections during the  
599 Omicron BA.1/2 wave.

### 600 **2. Laboratory methods**

#### 601 **2.1 Serum nAb titers against SARS-CoV-2 D614G and BA.1 variants (Lentiviral** 602 **Pseudovirus Production and Neutralization Assay)**

603 Virus production and pseudovirus neutralization assays were done as previously described<sup>48</sup>.  
604 Briefly, 293T/ACE2.MF cells modified to overexpress human ACE2 (kindly provided by M.  
605 Farzan (Scripps Research)) were cultured in DMEM (Gibco BRL Life Technologies) containing  
606 10% heat-inactivated serum (FBS) and 3  $\mu\text{g ml}^{-1}$  puromycin at 37 °C, 5% CO<sub>2</sub>. Cell monolayers  
607 were disrupted at confluency by treatment with 0.25% trypsin in 1 mM EDTA (Gibco BRL Life  
608 Technologies). The SARS-CoV-2, Wuhan-1 spike, cloned into pCDNA3.1 was mutated using the  
609 QuikChange Lightning Site-Directed Mutagenesis kit (Agilent Technologies) and NEBuilder  
610 HiFi DNA Assembly Master Mix (NEB) to include D614G (wild-type) or lineage defining  
611 mutations for Delta (T19R, 156-157del, R158G, L452R, T478K, D614G, P681R and D950N)  
612 and ), Omicron BA.1 (A67V, 69-70del, T95I, G142D, 143-145del, 211del, L212I, 214EPE,  
613 G339D, S371L, S373P, S375F, K417N, N440K, G446S, S477N, T478K, E484A, Q493R, G496S,  
614 Q498R, N501Y, Y505H, T547K, D614G, H655Y, N679K, P681H, N764K, D796Y, N856K,  
615 Q954H, N969K, L981F), Omicron BA.2 (T19I, L24S, 25-27del, G142D, V213G, G339D, S371F,  
616 S373P, S375F, T376A, D405N, R408S, K417N, N440K, S477N, T478K, E484A, Q493R,  
617 Q498R, N501Y, Y505H, D614G, H655Y, N679K, P681H, N764K, D796Y, Q954H, N969K).  
618 Pseudoviruses were produced by co-transfection in 293T/17 cells with a lentiviral backbone  
619 (HIV-1 pNL4.luc encoding the firefly luciferase gene) and either of the full-length SARS-CoV-2  
620 spike plasmids with PEIMAX (Polysciences). Culture supernatants were clarified of cells by a  
621 0.45 $\mu\text{m}$  filter and stored at -70 °C. Plasma samples were heat-inactivated and clarified by  
622 centrifugation. Pseudovirus and serially diluted plasma/sera were incubated for 1 h at 37 °C, 5%  
623 CO<sub>2</sub>. Cells were added at  $1 \times 10^4$  cells per well after 72 h of incubation at 37 °C, 5% CO<sub>2</sub>,  
624 luminescence was measured using PerkinElmer Life Sciences Model Victor X luminometer.  
625 Neutralization was measured as described by a reduction in luciferase gene expression after  
626 single-round infection of 293T/ACE2.MF cells with spike-pseudotyped viruses. Titers were  
627 calculated as the reciprocal plasma dilution (ID<sub>50</sub>) causing 50% reduction of relative light units.

628 Noting that we measured neutralization titer using a lentiviral-backboned pseudovirus  
629 neutralization assay. A systematic review of Omicron neutralization data showed that  
630 pseudovirus neutralization assays tend to report higher neutralizing titers compared to live-virus  
631 assays. The titer drops from wild type to Omicron also tend to be less pronounced for  
632 pseudovirus platforms, suggesting the pseudovirus assay may underestimate Omicron's  
633 capability to escape neutralization<sup>49</sup>.

634

## 635 **2.2 SARS-CoV-2 spike enzyme-linked immunosorbent assay (ELISA)**

636 For ELISA, Hexapro SARS-CoV-2 full spike protein with the D614G substitution was expressed  
637 in Human Embryonic Kidney (HEK) 293F suspension cells by transfecting the cells with the  
638 respective expression plasmid. After incubating for 6 days at 37°C, proteins were first purified  
639 using a nickel resin followed by size exclusion chromatography. Relevant fractions were  
640 collected and frozen at -80°C until use. Two µg/mL of D614G spike protein was used to coat 96-  
641 well, high-binding plates (Corning) and incubated overnight at 4°C. The plates were incubated in  
642 a blocking buffer consisting of 1x PBS, 5% skimmed milk powder, 0.05% Tween 20. Plasma  
643 samples were diluted to 1:100 starting dilution in a blocking buffer and added to the plates. IgG  
644 secondary antibody (Merck) was diluted to 1:3000 in blocking buffer and added to the plates  
645 followed by TMB substrate (Thermofisher Scientific). Upon stopping the reaction with 1 M  
646 H<sub>2</sub>SO<sub>4</sub>, optical density (OD) was measured at 450 nm. The monoclonal antibodies (mAbs)  
647 CR3022 and Palivizumab were used as the positive and negative controls respectively.

648

## 649 **3. Mediation analyses and household transmission model fitted to observed infections in the** 650 **cohort.**

651 Here we blend concepts from causal inference and infectious disease transmission models. The  
652 stability assumption in causal inference stipulates that the outcome of an individual does not  
653 depend on the outcome of others, which is often violated in infectious disease dynamics. This is  
654 because the spread of infectious diseases requires pathogens to be transmitted from one host to  
655 another. In other words, the infection outcome of one individual inherently depends on the  
656 infection outcome of others, and this is particularly pronounced in a household setting<sup>34</sup>. The  
657 “dependent happening” nature of infectious disease dynamics violates the stability assumption.  
658 As a result, the traditional regression approach for causal inference analysis cannot be applied to  
659 infectious disease outcomes among individuals who can in theory transmit the disease from one  
660 to another. To overcome this, Halloran, et al.<sup>34</sup> introduced the probability of infection  
661 conditional on exposure to already infected individuals (transmission probability), as the causal  
662 parameter. Using this proposed framework, we can investigate how the presence/absence of pre-

663 existing immunity along with the immunologic marker of interest could modulate probability of  
664 infection, after adjusting for levels of exposure to the infectious source(s). The corresponding  
665 causal inference framework requires modelling the transmission process explicitly. Under this  
666 framework, we conduct mediation analyses to investigate how nAb titers against variants at the  
667 start of a SARS-CoV-2 wave correlate with SARS-CoV-2 transmission risk, using the Delta and  
668 Omicron BA.1/2 waves as examples. We focus on the Delta and Omicron subgroup participants  
669 who have had a single or no prior infection. Specifically, we introduce the causal parameters:

- 670
- 671 •  $p_{ij}^k$ : the per-contact SARS-CoV-2 household transmission probability from infected  
672 individual  $i$  to individual  $j$  in household  $k$ .
  - 673 •  $q_j^k$ : the overall probability of acquiring SARS-CoV-2 infection from outside the  
674 household by individual  $j$  of household  $k$  (probability of infection from the community).

675 We use  $e_j$  to indicate individual  $j$ 's prior SARS-CoV-2 infection history, with  $e_j = 0$  representing  
676 no prior infection reported before the start of Delta/Omicron BA.1/2 and  $e_j = 1$  representing one  
677 prior infection by the start of Delta/Omicron BA.1/2 wave. A prior SARS-CoV-2 infection  
678 ( $e_j = 1$ ) would induce immunologic responses, measured by a set of immune markers (i.e.,  
679 candidate mediators)  $\{m_j|e_j = 1\}$  (e.g., nAb titers level). Then the household transmission  
680 probability  $p_{ij}^k = p_{ij}^k(e_j, \{m_j|e_j = 1\}, \{c_i, c_j, c_k\})$  can be expressed as a function of prior infection  
681 status  $e_j$ , immunologic mediators of SARS-CoV-2 transmission probability  $\{m_j|e_j = 1\}$  and  
682 additional adjustment terms  $\{c_i, c_j, c_k\}$ , representing a set of potential confounding factors of  
683 individual  $i$ , individual  $j$ , and household  $k$  (eg, age of the donor and/or recipient, comorbidities,  
684 household size, etc). Similarly, the community infection probability  $q_j^k = q_j^k(e_j, \{m_j|e_j =$   
685  $1\}, \{c_j\})$  can be expressed as a function of individual  $j$ 's prior exposure history  $e_j$ ,  
686 immunological markers  $\{m_j|e_j = 1\}$ , and additional adjustment terms  $\{c_j\}$ , representing a set of  
687 potential confounding factors of individual  $j$  (e.g., age or comorbidities).

688 The causal diagram of the mediation analysis framework is shown in Fig. 3. We fit a  
689 household transmission model to the imputed household transmission chains based on an  
690 Expectation-maximization (EM) algorithm (detailed in Section 4). Specifically, for the  
Delta/Omicron BA.1/2 wave, if we look into a specific household  $k$  of size  $N$ , there are a total of

691  $n$  individuals infected belonging to  $L$  distinct chains of transmission due to  $L$  independent  
692 introductions of SARS-CoV-2 into the household. The uninfected individuals are  $N - n$ . We  
693 denote  $P_j^k$  the likelihood of any individual  $j$  of household  $k$  having the observed infection status  
694 over the Delta/Omicron BA.1/2 wave (i.e., either infected or not) in a particular realization of the  
695 model. There are a few scenarios to write down  $P_j^k$ :

- 696 • Within a given transmission chain  $l \in L$ , the initial generation  $g_j^l = 0$  always has an  
697 individual  $j$  acquiring infection from the general community (outside the household  $k$ ).  
698 Thus, the probability of individual  $j$  being infected is  $P_j^k = q_j^k$  if  $j$  is the first individual  
699 to be infected in the chain.
- 700 • For infected individual  $j$  in the first generation of transmission chain  $l$ , i.e.,  $g_j^l = 1$ , this  
701 individual would have to escape infection risk from the general community but get  
702 infected by the infected household member of  $g_i^l = 0$ . Thus, the probability of individual  
703  $j$  being infected can be written as  $P_j^k = (1 - q_j^k)p_{ij}^k$ .
- 704 • For infected individual  $j$  in transmission chain  $l$  with generation greater than 1, i.e.,  
705  $g_l > 1$ , this individual has escaped infection risk from the general community as well as  
706 infected individuals  $i$  two generations away ( $g_i^l \leq g_j^l - 2$ ) but got infected by an infector  
707  $i^l$  of  $j$ 's previous generation on the same transmission chain  $l$ . Thus, the probability of  
708 individual  $j$  being infected can be written as  $P_j^k = (1 - q_j^k) \times \prod_{i \in \{g_i^l \leq g_j^l - 2\}} (1 - p_{ij}^k) \times$   
709  $p_{i^l j}^k$ .
- 710 • For uninfected individual  $j$  within household  $k$ , this individual has escaped infection risk  
711 from the general community as well as all the  $n$  infected individuals within the same  
712 household. Thus, the probability of individual  $j$  remaining uninfected can be written as  
713  $P_j^k = (1 - q_j^k) \times \prod_{i \in \{n\}} (1 - p_{ij}^k)$ .

714 Then, within household  $k$  of size  $N$ , we can express the likelihood of transmission chain  $l$  as  
715  $\prod_{j \in l} P_j^k$ ; the likelihood of observing all infections within  $k$  can be expressed as  $\prod_{l \in L} \prod_{j \in l} P_j^k$ ; the  
716 likelihood of observing  $N - n$  uninfected individuals can be expressed as  $\prod_{j \in N-n} P_j^k$ . Putting  
717 these together, the likelihood of observing one realization of the imputed (details of the EM

718 imputation method described in Section 4) households' transmission trees for Delta/Omicron  
 719 wave can be expressed as:

$$L^{Delta/Omicron} = \prod_k L_k^{Delta/Omicron} \quad \#(1)$$

720 Where the likelihood of a given household transmission chains configuration  $L_k^{Delta/Omicron}$  can  
 721 be expressed as:

$$L_k^{Delta/Omicron} = \prod_{l \in L} \prod_{j \in l} P_j^k(p_{ij}^k, q_j^k) \times \prod_{j \in N-n} P_j^k(p_{ij}^k, q_j^k) \quad \#(2)$$

722 In the remainder of the section, we will consider a few versions of the transmission model with  
 723 slightly different implementations for  $p_{ij}^k$  and  $q_j^k$ .

### 724 3.1 Model 1: waning model for prior exposure with serologically ascertained Delta and 725 Omicron wave infections.

726 This is the transmission model presented in the main analysis of the manuscript (results of the  
 727 model shown in Table 2. In this model, we consider that protection from prior infection  
 728 unexplained by nAb titers wanes over time but is not dependent on the variant responsible for  
 729 prior infection (i.e. prior D614G or Beta infections for the Delta wave analysis, and prior D614G,  
 730 Beta, or Delta infections for the Omicron wave analysis). Additionally, in this model, both the  
 731 Delta and Omicron wave infections were ascertained by serology based on approach describe in  
 732 Methods Section 1.

733 More specifically, for the Delta wave,  $p_{ij}^k$  and  $q_j^k$  can be expressed as:

$$p_{ij}^k = \text{expit} \left( \epsilon \left( \frac{1}{2} \right)^{\frac{\Delta t}{\tau}} e_j + \left( \delta_{nAb}^{D614G} m_j^{D614G} + o_{\Delta nAb}^{waning} m_j^{waning} \right) e_j + \lambda e_i + \sum_{c_i \in \{c_i\}} \gamma_{c_i} c_i + \sum_{c_j \in \{c_j\}} \gamma_{c_j} c_j + \sum_{c_k \in \{c_k\}} \gamma_{c_k} c_k + \alpha_s \right) \quad \#(3)$$

$$q_j^k = \text{expit} \left( \epsilon \left( \frac{1}{2} \right)^{\frac{\Delta t}{\tau}} e_j + \left( \delta_{nAb}^{D614G} m_j^{D614G} + o_{\Delta nAb}^{waning} m_j^{waning} \right) e_j + \sum_{c_j \in \{c_j\}} \gamma_{c_j} c_j + \sum_{c_k \in \{c_k\}} \gamma_{c_k} c_k + \beta_s \right) \quad \#(4)$$

734 As described before,  $e_j$  indicates individual  $j$ 's prior SARS-CoV-2 infection history, with  $e_j = 0$   
735 representing uninfected individuals at the start of the Delta wave,  $e_j = 1$  representing one prior  
736 infection, and  $\epsilon$  representing the effect size of the immune protection by prior infection not  
737 mediated through anti-D614G nAbs (direct effect, Table 2).  $\Delta t$  is the elapsed time between prior  
738 infection and blood draw 5 (the blood draw taken prior to the Delta wave which we use in this  
739 model) and  $\tau$  is the waning half-life of  $\epsilon$  (direct effect, Table 2).  $m_j^{D614G}$  represents the anti-  
740 D614G nAb titer at blood draw 5 and  $\delta_{nAb}^{D614G}$  represents the effect size of  $m_j^{D614G}$  in mediating  
741 infection probability  $p_{ij}^k$  against the Delta wave infection (mediator effect, Table 2) at blood draw  
742 5. While  $m_j^{waning}$  represents the quantity of anti-D614G nAbs waned from peak level (measured  
743 as the highest anti-D614G nAb titer level among the first 5 blood draws) to that at BD5 and  
744  $o_{\Delta nAb}^{waning}$  represents the effect size of  $m_j^{waning}$  in mediating transmission probability  $p_{ji}^k$  against  
745 the Delta wave infection (mediator effect, Table 2) at blood draw 5. Note that the term  
746  $\delta_{nAb}^{D614G} m_j^{D614G} + o_{\Delta nAb}^{waning} m_j^{waning}$  only exists when  $e_j = 1$ .

747 We further evaluate whether breakthrough infections have reduced infectiousness compared to  
748 primary infections and may in turn affect  $p_{ij}^k$ . We use  $e_i$  to indicate individual  $i$ 's (the donor)  
749 prior SARS-CoV-2 infection history ( $e_i = 0$  means no infection, and  $e_i = 1$  represents one prior  
750 infection at the start of Delta wave). Further,  $\lambda$  represents the effect size of prior infection (in  $i$ )  
751 in reducing the infectiousness of reinfections.

752 We also consider confounding factors for donor  $i$  and recipient  $j$ , where  $c_i$  and  $\gamma_{c_i}$  represent  
753 infector  $i$ 's confounding factor ( $i$ 's age, sex) and effect size, respectively;  $c_j$  and  $\gamma_{c_j}$  represent  $j$ 's  
754 confounding factor ( $j$ 's age/sex-specific susceptibility (biology), age/sex- and site-specific  
755 susceptibility (behavioral), HIV infection status) and effect size, respectively;  $c_k$  and  $\gamma_{c_k}$   
756 represent household  $k$ 's confounding factor (household size) and effect size, respectively. Lastly,  
757  $\alpha_s$  and  $\beta_s$  are logits of the baseline risks for household and community exposures. All parameters'  
758 effect sizes are measured in the log of odds ratios.

759 Similarly, for the Omicron BA.1/2 wave,  $p_{ij}^k$  and  $q_j^k$  can be expressed as:

$$p_{ij}^k = \text{expit} \left( \begin{aligned} &\epsilon \left( \frac{1}{2} \right)^{\frac{\Delta t}{\tau}} e_j + (o_{nAb}^{BA1} m_j^{BA1} + o_{\Delta nAb}^{escape} m_j^{escape}) e_j + \lambda e_i + \\ &\sum_{c_i \in \{c_i\}} \gamma_{c_i} c_i + \sum_{c_j \in \{c_j\}} \gamma_{c_j} c_j + \sum_{c_k \in \{c_k\}} \gamma_{c_k} c_k + \alpha_s \end{aligned} \right) \#(5)$$

$$q_j^k = \text{expit} \left( \begin{aligned} &\epsilon \left( \frac{1}{2} \right)^{\frac{\Delta t}{\tau}} e_j + (o_{nAb}^{BA1} m_j^{BA1} + o_{\Delta nAb}^{escape} m_j^{escape}) e_j + \\ &\sum_{c_j \in \{c_j\}} \gamma_{c_j} c_j + \sum_{c_k \in \{c_k\}} \gamma_{c_k} c_k + \beta_s \end{aligned} \right) \#(6)$$

760 As described before,  $e_j$  indicates individual  $j$ 's prior SARS-CoV-2 infection history, with  $e_j = 0$   
 761 representing individual  $j$  remained naïve to SARS-CoV-2 at the start of Omicron BA.1/2 wave  
 762 while  $e_j = 1$  representing individual  $j$  had one prior infection at the start of Omicron BA.1/2  
 763 wave and  $\epsilon$  represents the effect size of the immune protection by prior infection not mediated  
 764 through anti-D614G nAbs (direct effect, Table 2).  $\Delta t$  is the elapsed time between prior infection  
 765 and blood draw 8 (the blood draw taken prior to the Omicron BA.1/2 wave) and  $\tau$  is the waning  
 766 half-life of  $\epsilon$  (direct effect, Table 2). Here we consider that parameter  $\tau$  is shared between the  
 767 Delta and Omicron wave and will be jointly estimated (described in Methods Section 4).  $m_j^{BA1}$   
 768 represents the anti-BA1 nAb titer at blood draw 8 and  $o_{nAb}^{BA1}$  represents the effect size of  $m_j^{BA1}$  in  
 769 mediating transmission probability  $p_{ji}^k$  against the Omicron BA.1/2 wave infection (mediator  
 770 effect, Table 2) at blood draw 8. While  $m_j^{escape}$  represents the difference in titer from anti-  
 771 D614G nAb to anti-BA1 nAb at blood draw 8 and  $o_{\Delta nAb}^{escape}$  represents the effect size of  $m_j^{escape}$   
 772 in mediating transmission probability  $p_{ji}^k$  against the Omicron BA.1/2 wave infection (mediator  
 773 effect, Table 2) at blood draw 8. Note that the term  $o_{nAb}^{BA1} m_j^{BA1} + o_{\Delta nAb}^{escape} m_j^{escape}$  only exists  
 774 when  $e_j = 1$ . All other parameters have the same definition of the Delta wave.

775  $\alpha_s, \beta_s, \epsilon, \tau, o_{\Delta nAb}^{escape}, o_{nAb}^{BA1}, \{\gamma_{c_i}\}, \{\gamma_{c_j}\}, \{\gamma_{c_k}\}$  are estimated through maximizing the likelihood  
 776 function  $L$  for each of the 100 bootstrapped realizations and bootstrap mean and confidence  
 777 intervals are calculated for each of the parameters.

778 **3.2 Model 2: Sensitivity analysis considering variant-specific prior exposure for the direct**  
 779 **effects.**



780 A potential confounding factor in understanding the waning of protection through direct effects is  
 781 the diversity of prior SARS-CoV-2 exposures, with the dominance of D614G variant in the first  
 782 wave, Beta variant in the second wave, and Delta variant in the third wave (Fig. 1). The  
 783 effectiveness of protection may vary depending on the specific variant of prior exposure that  
 784 induced the immune response at play. We conducted a sensitivity analysis (Model 2) employing a  
 785 variant-specific model for the direct effects, which accounted for distinct types of SARS-CoV-2  
 786 variants conferring prior immunity, instead of considering generic a waning model. Specifically,  
 787 in Model 2, we considered a more complex version of Model 1, where protection from prior  
 788 infection depends on the type of infecting variant (i.e. prior D614G or Beta infections for the  
 789 Delta wave analysis, and prior D614G, Beta, or Delta infections for the Omicron wave analysis).  
 790 We consider waning in neutralizing titers as in Model 1, but we eliminate waning in the effect of  
 791 prior infection that is not captured by neutralizing titers. More specifically, for the Delta wave,  
 792  $p_{ij}^k$  and  $q_j^k$  can be expressed as:

$$p_{ij}^k = \text{expit} \left( \begin{array}{c} \epsilon^{D614G} e_j^{D614G} + \epsilon^{Beta} e_j^{Beta} + \left( \delta_{nAb}^{D614G} m_j^{D614G} + o_{\Delta nAb}^{waning} m_j^{waning} \right)^{e_j} + \lambda e_i + \\ \sum_{c_i \in \{c_i\}} \gamma_{c_i} c_i + \sum_{c_j \in \{c_j\}} \gamma_{c_j} c_j + \sum_{c_k \in \{c_k\}} \gamma_{c_k} c_k + \alpha_s \end{array} \right) \#(7)$$

$$q_j^k = \text{expit} \left( \begin{array}{c} \epsilon^{D614G} e_j^{D614G} + \epsilon^{Beta} e_j^{Beta} + \left( \delta_{nAb}^{D614G} m_j^{D614G} + o_{\Delta nAb}^{waning} m_j^{waning} \right)^{e_j} + \\ \sum_{c_j \in \{c_j\}} \gamma_{c_j} c_j + \sum_{c_k \in \{c_k\}} \gamma_{c_k} c_k + \beta_s \end{array} \right) \#(8)$$

793  
 794 Here,  $e_j^{D614G(Beta)} = 1$  indicates individual  $j$ , prior to the Delta wave, was infected with D614G  
 795 (Beta) variant. If  $e_j^{D614G} = e_j^{Beta} = 0$ , individual  $j$  was naïve at the beginning of the Delta wave.  
 796  $\epsilon^{D614G}$  and  $\epsilon^{Beta}$  represent the effect size of immune protection by prior D614G and Beta  
 797 infection not mediated through anti-D614G nAbs, respectively.

798 For the Omicron wave,  $p_{ij}^k$  and  $q_j^k$  can be expressed as:

$$p_{ij}^k = \text{expit} \left( \begin{array}{c} \epsilon^{D614G} e_j^{D614G} + \epsilon^{Beta} e_j^{Beta} + \epsilon^{Delta} e_j^{Delta} + \left( o_{nAb}^{BA1} m_j^{BA1} + o_{\Delta nAb}^{escape} m_j^{escape} \right)^{e_j} + \lambda e_i + \\ \sum_{c_i \in \{c_i\}} \gamma_{c_i} c_i + \sum_{c_j \in \{c_j\}} \gamma_{c_j} c_j + \sum_{c_k \in \{c_k\}} \gamma_{c_k} c_k + \alpha_s \end{array} \right) \#(9)$$

$$q_j^k = \text{expit} \left( \epsilon^{D614G} e_j^{D614G} + \epsilon^{Beta} e_j^{Beta} + \epsilon^{Delta} e_j^{Delta} + (o_{nAb}^{BA1} m_j^{BA1} + o_{\Delta nAb}^{escape} m_j^{escape})^{e_j} + \sum_{c_j \in \{c_j\}} \gamma_{c_j} c_j + \sum_{c_k \in \{c_k\}} \gamma_{c_k} c_k + \beta_s \right) \#(10)$$

799 Here,  $e_j^{D614G(Beta,Delta)} = 1$  indicates individual  $j$ , prior to the Omicron wave, was infected with  
 800 D614G (Beta, Delta) variant. If  $e_j^{D614G} = e_j^{Beta} = e_j^{Delta} = 0$ , individual  $j$  was naïve at the  
 801 beginning of the Omicron wave.  $\epsilon^{D614G}$ ,  $\epsilon^{Beta}$  and  $\epsilon^{Delta}$  represent the effect size of the immune  
 802 protection by prior D614G, Beta and Delta infection not mediated through anti-D614G nAbs,  
 803 respectively.

804 Additionally, similarly to Model 1, both the Delta and Omicron wave infections were ascertained  
 805 by serology for Model 2. All other settings of Model 2 were kept the same as Model 1. The  
 806 results of the Model 2 are presented in Extended Data Table 2.

807 Our analysis revealed that for both the Delta and Omicron waves, more recent variants  
 808 conferred stronger protection than earlier variants, albeit with overlapping confidence intervals  
 809 (Extended Data Table 2). This temporal trend aligns with the expectations of the waning model.  
 810 Both waning and variant-specific immunity may modulate the direct effects of prior immunity;  
 811 however, our study lacked sufficient statistical power to jointly estimate the relative  
 812 contributions of these two factors. Full estimates of this sensitivity analyses are presented in  
 813 Extended Data Table 2.

814

### 815 **3.3 Model 3: Sensitivity analysis with Delta wave infections ascertained by PCR and/or** 816 **serology.**

817 For Model 1, both the Delta and Omicron wave infection outcomes were inferred using the  
 818 kinetics of anti-nucleocapsid antibodies from longitudinal serologic sampling, as detailed in  
 819 previously published studies of the PHIRST-C cohort<sup>30,32</sup>. This approach for inferring infections  
 820 based on serology was calibrated against virological evidence of infection during the Delta wave,  
 821 established through twice-weekly rRT-PCR tests regardless of symptom presentation. However,  
 822 it should be noted that this calibration did not achieve perfect concordance; the serology  
 823 approach demonstrated 93% sensitivity and 89% specificity when compared to infections  
 824 identified by rRT-PCR tests<sup>30</sup>. To address the uncertainties arising from the imperfect

825 concordance between the two approaches for ascertaining infections, we conducted a sensitivity  
 826 analysis (Model 3) for the Delta wave, where we considered infections based on rRT-PCR  
 827 positivity and/or anti-nucleocapsid antibody serology. We identified an additional 17 infections  
 828 during the Delta wave through this more sensitive infection ascertainment approach, bringing the  
 829 total number of Delta wave infections to 290. All other settings of Model 3 were kept the same as  
 830 Model 1. The results of the Model 3 are presented in Extended Data Table 3.

831 Notably, estimates of the direct and indirect effects of the mediation analysis were comparable  
 832 between this sensitivity analysis and the main analysis (compare Extended Data Table 3 to Table  
 833 1). These findings provide support for the utilization of anti-nucleocapsid serology to ascertain  
 834 Omicron BA.1/2 wave infections in the studied cohorts, in a period where twice-weekly rRT-  
 835 PCR testing was not available and confirms the robustness of our CoP analyses.

836

### 837 **3.4 Model 4: D614G spike binding antibodies as mediators of protection.**

838 We conducted sensitivity analysis (Model 4) to explore the role of D614G spike binding  
 839 antibodies (referred to as bAb hereafter), as potential correlates of protection for both Delta and  
 840 Omicron infections. Employing an in-house enzyme-linked immunosorbent assay (ELISA), we  
 841 quantified the level of D614G spike bAb based by measuring absorbance at 450nm at an optical  
 842 density (OD) at peak levels and BD5 (DB8) for the Delta (Omicron) wave analysis (Extended  
 843 Data Fig. 3). The reduction in binding antibody levels from peak ( $\Delta bAb^W$ ) was determined as the  
 844 difference between OD values at peak and BD5 (BD8) for the Delta (Omicron) wave (Extended  
 845 Data Fig. 3).

846 Model 4 builds on Model 2 but replaces nAb titers with D614G spiking binding ELISA readouts  
 847 as mediators of protection, in order to compare the protection afforded by neutralizing vs binding  
 848 antibodies. More specifically, for the Delta wave,  $p_{ij}^k$  and  $q_j^k$  can be expressed as:

$$p_{ij}^k = \text{expit} \left( \epsilon^{D614G} e_j^{D614G} + \epsilon^{Beta} e_j^{Beta} + \left( \delta_{bAb}^{D614G} m_j^{D614G} + o_{\Delta bAb}^{waning} m_j^{waning} \right)^{e_j} + \lambda e_i + \sum_{c_i \in \{c_i\}} \gamma_{c_i} c_i + \sum_{c_j \in \{c_j\}} \gamma_{c_j} c_j + \sum_{c_k \in \{c_k\}} \gamma_{c_k} c_k + \alpha_s \right) \#(11)$$

$$q_j^k = \text{expit} \left( \frac{\epsilon^{D614G} e_j^{D614G} + \epsilon^{Beta} e_j^{Beta} + \left( \delta_{bAb}^{D614G} m_j^{D614G} + o_{\Delta bAb}^{waning} m_j^{waning} \right)^{e_j} + \sum_{c_j \in \{c_j\}} \gamma_{c_j} c_j + \sum_{c_k \in \{c_k\}} \gamma_{c_k} c_k + \beta_s}{\sum_{c_j \in \{c_j\}} \gamma_{c_j} c_j + \sum_{c_k \in \{c_k\}} \gamma_{c_k} c_k + \beta_s} \right) \#(12)$$

849

850 Here,  $m_j^{D614G}$  represents the D614G spike binding antibodies ELISA readout at blood draw 5  
 851 and  $\delta_{bAb}^{D614G}$  represents the effect size of  $m_j^{D614G}$  in mediating transmission probability  $p_{ij}^k$   
 852 against the Delta wave infection at blood draw 5. Further,  $m_j^{waning}$  represents the drop from  
 853 peak D614G spike binding antibodies readout prior to blood draw 5 (measured as the highest  
 854 D614G spike binding Ab titer level among the first 5 blood draws) to that at blood draw 5 and  
 855  $o_{\Delta bAb}^{waning}$  represents the effect size of  $m_j^{waning}$  in mediating transmission probability  $p_{ji}^k$  against  
 856 the Delta wave infection at blood draw 5.

857 For the Omicron wave,  $p_{ij}^k$  and  $q_j^k$  can be expressed as:

$$p_{ij}^k = \text{expit} \left( \frac{\epsilon^{D614G} e_j^{D614G} + \epsilon^{Beta} e_j^{Beta} + \epsilon^{Delta} e_j^{Delta} + \left( \delta_{bAb}^{D614G} m_j^{D614G} + o_{\Delta bAb}^{waning} m_j^{waning} \right)^{e_j} + \lambda e_i + \sum_{c_i \in \{c_i\}} \gamma_{c_i} c_i + \sum_{c_j \in \{c_j\}} \gamma_{c_j} c_j + \sum_{c_k \in \{c_k\}} \gamma_{c_k} c_k + \alpha_s}{\sum_{c_i \in \{c_i\}} \gamma_{c_i} c_i + \sum_{c_j \in \{c_j\}} \gamma_{c_j} c_j + \sum_{c_k \in \{c_k\}} \gamma_{c_k} c_k + \alpha_s} \right) \#(13)$$

$$q_j^k = \text{expit} \left( \frac{\epsilon^{D614G} e_j^{D614G} + \epsilon^{Beta} e_j^{Beta} + \epsilon^{Delta} e_j^{Delta} + \left( \delta_{bAb}^{D614G} m_j^{D614G} + o_{\Delta bAb}^{waning} m_j^{waning} \right)^{e_j} + \sum_{c_j \in \{c_j\}} \gamma_{c_j} c_j + \sum_{c_k \in \{c_k\}} \gamma_{c_k} c_k + \beta_s}{\sum_{c_j \in \{c_j\}} \gamma_{c_j} c_j + \sum_{c_k \in \{c_k\}} \gamma_{c_k} c_k + \beta_s} \right) \#(14)$$

858 Here,  $m_j^{D614G}$  represents the D614G spike binding antibodies ELISA readout at blood draw 8  
 859 and  $\delta_{bAb}^{D614G}$  represents the effect size of  $m_j^{D614G}$  in mediating transmission probability  $p_{ij}^k$   
 860 against the Omicron wave infection at blood draw 8. While  $m_j^{waning}$  represents the drop from  
 861 peak D614G spike binding antibodies readout prior to blood draw 8 (measured as the highest  
 862 D614G spike binding Ab titer level among the first 8 blood draws) to that at blood draw 8 and  
 863  $o_{\Delta bAb}^{waning}$  represents the effect size of  $m_j^{waning}$  in mediating transmission probability  $p_{ji}^k$  against  
 864 the Omicron wave infection at blood draw 8. All other settings of Model 4 were kept the same as  
 865 Model 2. The results of the Model 4 are presented in Extended Data Table 4.

866 We found that binding antibody levels at BD5 (BD8) correlate with protection against Delta  
867 (Omicron) wave infections: the risk of infection decreased by 74% (95% CI 41% – 88%) and 40%  
868 (95% CI 33% – 54%) per unit increase in OD value for the Delta and Omicron wave analyses,  
869 respectively. Conversely, the decline in bAbs from peak levels to BD5/BD8 ( $\Delta bAb^W$ )  
870 demonstrated no contribution to the overall protection, with risk reduction per 10-fold increase: -  
871 2% (95%CI: -91% – 55%) for Delta wave infections and -2% (95%CI: -87% – 55%) for  
872 Omicron wave infections. These findings underscore the correspondence between waning of  
873 binding antibodies and a waning of protection. Furthermore, our estimations indicate that the  
874 proportion of protection conferred through D614G spike bAbs at BD5 is 35% (95%CI: 32% –  
875 38%) against Delta wave infections, a figure comparable estimation based on anti-D614G nAbs  
876 (37%, 95%CI: 34% – 40%, Extended Data Table 4). Notably, D614G spike bAbs at BD8  
877 accounted for 27% (95% CI: 25% – 29%) of protection against Omicron wave infection,  
878 representing a larger proportion compared to anti-BA.1 nAbs (11%, 95%CI: 9% – 12%,  
879 Extended Data Table 4).

880

#### 881 **4. Transmission chains imputation and parameters estimation based on an Expectation-** 882 **maximization (EM) algorithm.**

883 Here we describe the process to fit the models described in Section 3 to the household infection  
884 data. The serologic data available for the Delta and Omicron only provides information on the  
885 total number of infections within the household between two blood draws collected before and  
886 after the SARS-CoV-2 wave. The data does not provide the details of the transmission chains  
887 within the household, the order of infections among infected individuals, nor the infection dates.  
888 To account for the uncertainties of the transmission tree structure within households given only  
889 the total number of infections, we enumerate and reconstruct all possible transmission chains  
890 among the infected individuals, where each infected individual may have been infected by  
891 members of their own household or the general community. Supplementary Fig. 1 illustrates all  
892 16 possible configurations of transmission chains for a household with 3 infected individuals. We  
893 limited our analysis to households with no more than 6 infected individuals, as the possible  
894 configurations of transmission chains among 6 infected individuals already reaches 16,807.  
895 Enumeration of all possible transmission chain configurations would be computationally

896 intractable for households with more than 6 infected individuals. Additionally, the probability of  
897 each possible transmission chain depends on the parameter estimates of the transmission model  
898 described in Methods Section 3. To address the statistical uncertainties due to unresolved  
899 transmission chains (which would affect the statistical confidence of mediation analysis detailed  
900 in the prior section), we jointly fit the household transmission model and impute the topological  
901 structure of the transmission trees. We use an EM algorithm, as described below.

902 To resolve who infected whom within the household in a probabilistic manner, we considered an  
903 EM algorithm that iteratively estimates the transmission model parameters  $\alpha_s$ ,  $\beta_s$ ,  $\epsilon$ ,  $\tau$ ,  
904  $\delta_{nAb}^{D614G/BA1}$ ,  $o_{\Delta nAb}^{waning/escape}$ ,  $\{\gamma_{c_i}\}$ ,  $\{\gamma_{c_j}\}$ ,  $\{\gamma_{c_k}\}$  through maximizing the likelihood function  $L$  as  
905 described in Equation (1) in the previous section then updates the imputed probability of each  
906 transmission tree configuration within each household based on the fitted transmission model.  
907 The process is as follows:

- 908 (1) Initial imputation of the household transmission trees with equal sampling probability for  
909 all configurations: For each household, we randomly sample one transmission tree with  
910 equal probability among all transmission tree configurations that are compatible with the  
911 number of infections. We iterate through all households so that each household has a  
912 simulated transmission tree. We then repeat the imputation 1000 times to obtain 1000  
913 realizations of each household's transmission tree.
- 914 (2) Maximization step: We consider the waning parameter  $\tau$  a hyper-parameter (nonlinear  
915 term in equations (3-6), cannot be estimated by logistic regression). For a fixed value of  $\tau$ ,  
916 for each of the 1000 realizations of the simulated household transmission chains, we  
917 estimate transmission model parameters  $\alpha_s$ ,  $\beta_s$ ,  $\epsilon$ ,  $\delta_{nAb}^{D614G/BA1}$ ,  $o_{\Delta nAb}^{waning/escape}$ ,  $\{\gamma_{c_i}\}$ ,  
918  $\{\gamma_{c_j}\}$ ,  $\{\gamma_{c_k}\}$  through maximizing the likelihood function  $L$  described in Equation (1). The  
919 maximization of the likelihood function is achieved through fitting a logistic regression  
920 of the infection/exposure outcomes for all participants using R package "**brglm**" (version  
921 0.7.2). We then pool the estimates from the 1000 realizations using the "**pool**" function in  
922 the R package "**mice**" (version 3.16.0). The full likelihood of the combined Delta and  
923 Omicron waves fitting in this EM step  $m$  can be expressed as  $L_m(\tau) = L_m^{Delta}(\tau) \times$   
924  $L_m^{Omicron}(\tau)$

- 925 (3) Expectation step: for a fixed value of hyper-parameter  $\tau$ , based on the pooled estimates of  
926 the transmission model parameters  $\alpha_s, \beta_s, \epsilon, \delta_{nAb}^{D614G/BA1}, o_{\Delta nAb}^{waning/escape}, \{\gamma_{c_i}\}, \{\gamma_{c_j}\},$   
927  $\{\gamma_{c_k}\}$ , we calculate the likelihood all configurations of transmission chains within each  
928 household based on Equation (2). We use these configuration-specific likelihoods to  
929 resample transmission chains: For each household, we randomly sample one transmission  
930 tree among all transmission tree configurations with probability proportional to  
931 transmission tree likelihood prescribed in Equation (2), given the parameters estimated by  
932 the most recent maximization step. We iterate through all households so that each  
933 household is assigned one simulated transmission tree. We repeat the process 1000 times  
934 to obtain 1000 realizations of the household transmission trees.
- 935 (4) For each of the fixed value of hyper-parameter  $\tau$  over a plausible range (30 - 500 days),  
936 we iterate over the EM steps (2) and (3) until  $L_m(\tau)$  converge to the maximum value of  
937 the EM algorithm. We scan through the values of  $\tau$  from 30 to 500 days at 10 days step.  
938 The EM algorithm convergence curve is shown in Supplementary Fig. 2 for each of the  $\tau$   
939 values. The EM algorithm converges at step 50, irrespective of the value of  $\tau$ . The  
940 marginal likelihood of the model at  $\tau$ ,  $L(\tau)$  is estimated by taking the average of  $L_m(\tau)$   
941 for EM steps 50 through 100. Supplementary Fig. 3 shows the log of the likelihood  $L(\tau)$   
942 as a function of  $\tau$ , based on a spline interpolation. The point estimate of  $\tau$  is taken from  
943 the maximum of  $\log(L(\tau))$  while the 95% confidence interval is estimated by finding  $\tau$   
944 values with log-likelihood value at the maximum minus 1.92 (Supplementary Fig. 3).
- 945 (5) We then take the best estimate of hyper-parameter  $\tau$  and repeat the EM algorithm till  
946 convergence to estimate transmission model parameters  $\alpha_s, \beta_s, \epsilon, \delta_{nAb}^{D614G/BA1},$   
947  $o_{\Delta nAb}^{waning/escape}, \{\gamma_{c_i}\}, \{\gamma_{c_j}\}, \{\gamma_{c_k}\}$  as show in Table 2. Same EM algorithm were applied to  
948 Model 2-4 for the sensitivity analysis as well.

949 The “treatment effect” by prior infection is estimated by simulating from the best-fit model. We  
950 first sample 1000 realizations of the imputed household transmission trees, with imputation  
951 probability proportional to the best estimates of transmission model using the EM algorithm and  
952 hyper-parameter  $\tau$ . For each of the 1000 realizations, we focus on the subset of individuals who  
953 had one prior SARS-CoV-2 infection, denoted as  $S_j = \{j | e_j = 1\}$ ). We use the fitted

954 transmission model to predict the probability of infection (i.e.  $P_j = p_{ij}^k$  or  $q_j^k$ , with ) of these  
955 non-naïve subsets under three scenarios:

- 956 a. Scenario 1: the probability of infection estimated with predictors as reported in  
957 the data, denoted as  $P_j^{obs}$ .
- 958 b. Scenario 2: a counterfactual scenario where the probability of infection is  
959 estimated with predictor  $e_j = 0$  (i.e. a counterfactual naïve individual) whereas all  
960 other covariates (confounders) are the same as observed, removing both direct and  
961 mediator effects. We denote the infection probability in this counterfactual  
962 scenario as  $P_j^{counterfactual}(e_j = 0)$ .
- 963 c. Scenario 3: a counterfactual scenario where the probability of infection is  
964 estimated with predictor  $e_j = 1$ , but setting  $m_{nAb}^{BA1} = 0$  (or  $m_{nAb}^{D614G} = 0$ ),  
965 effectively removing the mediator effect of nAb on preventing transmission, but  
966 keeping the direct effect. We denote the infection probability in this counterfactual  
967 scenario as  $P_j^{counterfactual}(e_j = 1; m_{nAb} = 0)$ .

968 We then calculate the total protection conferred by prior infection as the population average of  
969  $P_j^{counterfactual}(e_j = 0)/P_j^{obs}$ , based on bootstrap resampling with replacement (maintaining the  
970 same number of observations) of each of the 1000 realizations of the household transmission  
971 chains. Point estimates and 95% confidence intervals are based on the median and 95% quantiles  
972 of 1000 realizations' estimates.

973 Similarly, we calculate the proportion of protection mediated by nAbs as the population average  
974 of  $1 - \frac{P_j^{counterfactual}(e_j=1; m_{nAb}=0)/P_j^{obs}}{P_j^{counterfactual}(e_j=0)/P_j^{obs}}$ . We use the same bootstrapping approach as for total  
975 protection.

976



977 **Data availability**

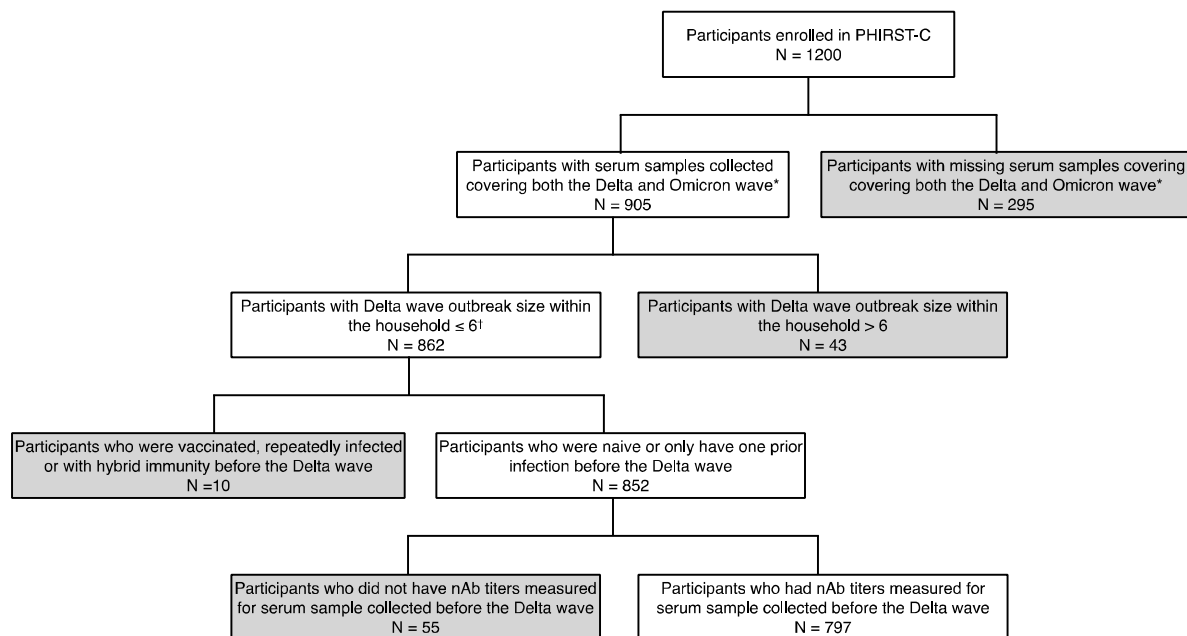
978 Aggregate data to reproduce the figures are available at Zenodo (DOI:  
979 [10.5281/zenodo.11375487](https://doi.org/10.5281/zenodo.11375487)). Individual-level data cannot be publicly shared because of ethical  
980 restrictions and the potential for identifying included individuals. Accessing individual  
981 participant data and a data dictionary defining each field in the dataset would require provision  
982 of protocol and ethics approval for the proposed use. To request individual participant data  
983 access, please submit a proposal to C.C. who will respond within 1 month of request. Upon  
984 approval, data can be made available through a data sharing agreement.

985 **Code availability**

986 Code to reproduce the figures, using python version 3.8.11 and scipy version 1.7.1 is available at  
987 Zenodo (DOI: [10.5281/zenodo.11375487](https://doi.org/10.5281/zenodo.11375487)).

988 **Extended Data Figures:**

989

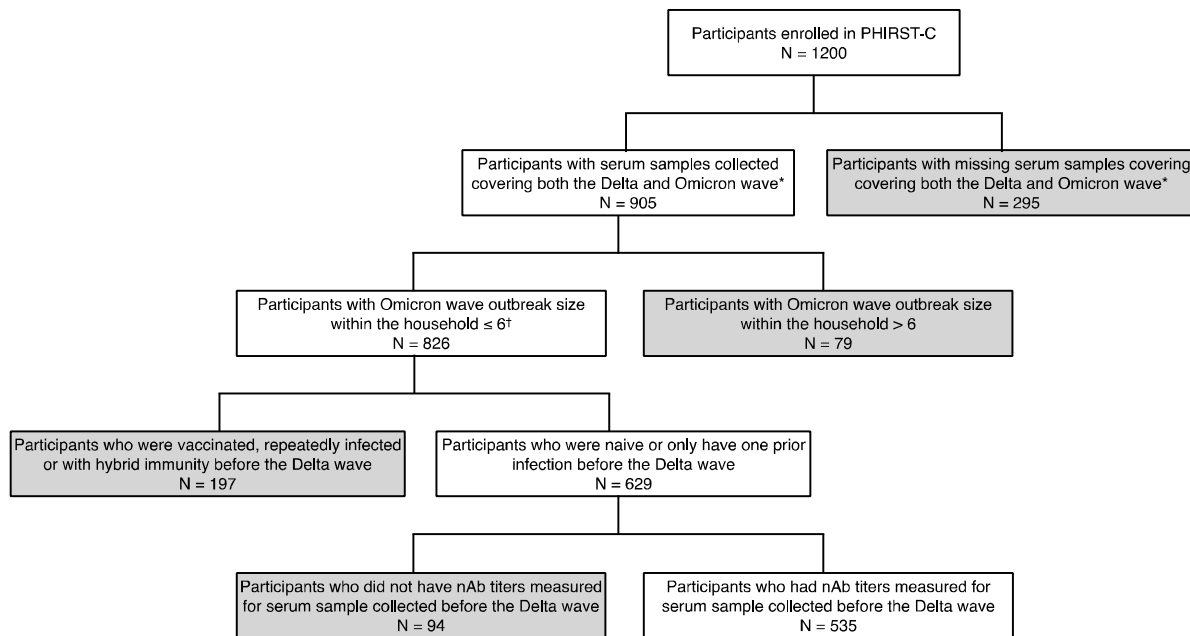


990 **Extended Data Fig. 1:** Flowchart of participants included in the Delta-wave subgroup analysis. Grey boxes  
991 represent participants excluded from the Delta-wave subgroup analysis.  
992

993 \*Based on a previously published study <sup>30</sup>.

994 †Household with more than 6 infected individuals would be computationally intractable to track all possible  
995 transmission chain configurations (Material and Methods Section 3).

996



997

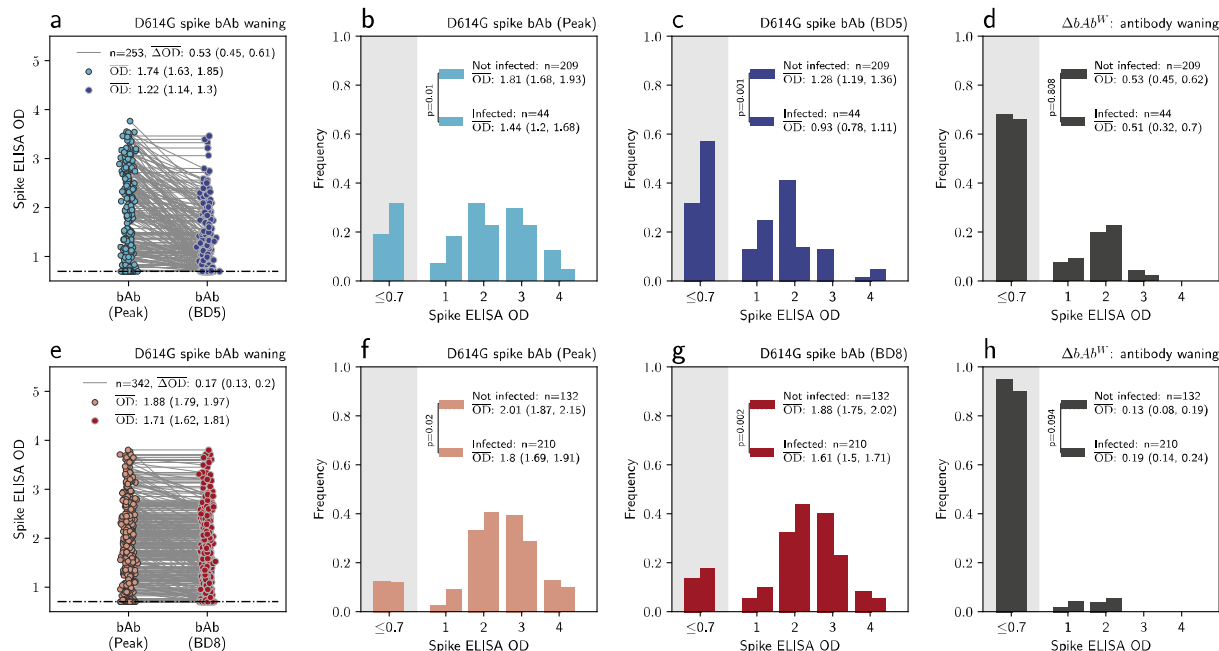
998 **Extended Data Fig. 2:** Flowchart of participants included in the Omicron-wave subgroup analysis. Grey boxes

999 represent participants excluded from the Omicron-wave subgroup analysis.

1000 \*Based on a previously published study<sup>30</sup>.

1001 †Household with more than 6 infected individuals would be computationally intractable to track all possible  
1002 transmission chain configurations (Material and Methods Section 3).

1003



1004

1005 **Extended Data Fig. 3: D614G spike binding antibody (bAb) level for the Delta wave and the Omicron wave**  
 1006 **analysis.** **a**, for Delta wave subgroup, the distribution of the peak bAb level to BD5 (light blue dots) and the D614G  
 1007 spike bAb level at BD5 (dark blue dots), among individuals who had one prior SARS-CoV-2 infection before blood  
 1008 draw 5. Each dot represents one individual, with two measurements of the same individual connected through a gray  
 1009 line. OD: absorbance at 450 nm, measured in optical density;  $\overline{OD}$ : the average of OD;  $\overline{\Delta OD}$ : the average drop of OD.  
 1010 **b**, for Delta wave subgroup, the distribution of the peak D614G spike bAb up to BD5, stratified by individuals who  
 1011 were infected during the Delta wave (solid bar) vs those who were not infected (dashed bar). Independent samples t-  
 1012 test (two-sided) is used to determine the statistical significance (anti reported on the legend) of difference between  
 1013 the  $\overline{OD}$  of the two groups. **c**, same as **b** but for D614G spike bAb level at BD5. **d**, same as **b** but for  $\Delta bAb^W$ . **e**, for  
 1014 Omicron wave subgroup, the distribution of the peak bAb level to BD8 (light red dots) and the D614G spike bAb  
 1015 level at BD8 (dark red dots), among individuals who had one prior SARS-CoV-2 infection before BD8. Each dot  
 1016 represents one individual, with two measurements of the same individual connected through a gray line. **f**, for the  
 1017 Omicron wave subgroup, the distribution of the D614G spike bAb level at BD8, stratified by individuals who were  
 1018 infected during the Omicron wave (solid bar) vs those who were not infected (dashed bar). Independent samples t-  
 1019 test (two-sided) is used to determine the statistical significance (p-value reported on the legend) of difference  
 1020 between the  $\overline{OD}$ s of the two groups. **g**, same as **f** but for D614G spike bAb level at BD8. **d**, same as **f** but for  $\Delta bAb^W$ .

1021

1022 **Extended Data Tables:**

1023 **Extended Data Table 1: Positivity rate of different serologic assays by the variant type of prior exposure for**  
 1024 **the Delta and Omicron wave subgroup.**

<b>Delta wave subgroup</b>			
<b>Seropositivity</b>	<b>Prior D614G infection</b>	<b>Prior Beta infection</b>	<b>Prior Delta exposure</b>
Anti-nucleocapsid assay were positive in at least one of the first 5 blood draws	109/113 (97%)	133/140 (95%)	–
Anti-nucleocapsid assay were positive at BD5	104/113 (92%)	129/140 (92%)	–
Anti-D614G nAb assay were positive for peak nAb response.	87/113 (77%)	60/140 (43%)	
Anti-D614G nAb were positive for nAb response at BD5	81/113 (72%)	59/140 (42%)	–
<b>Omicron wave subgroup</b>			
<b>Seropositivity</b>	<b>Prior D614G exposure</b>	<b>Prior Beta exposure</b>	<b>Prior Delta exposure</b>
Anti-nucleocapsid assay were positive in at least one of the first 8 blood draws	60/61 (98%)	116/120 (97%)	160/161 (99%)
Anti-nucleocapsid assay were positive at BD8	58/61 (95%)	108/120 (90%)	159/161 (99%)
Anti-D614G nAb were positive for nAb response at BD8	57/61 (93%)	71/120 (59%)	140/161 (87%)
Anti-BA.1 nAb were positive for nAb response at BD8	29/61 (48%)	36/120 (30%)	50/161 (31%)

1025

1026 **Extended Data Table 2: Mediation analysis for nAbs as CoPs against serologically ascertained Delta and**  
 1027 **Omicron wave infections, with a variant-specific model for direct effect.** Average and 95% CIs are provided for  
 1028 each of the model parameters.  $\Delta nAb^W$ : the quantity of anti-D614G nAbs waned from peak level to that at BD5.  
 1029  $\Delta nAb^E$ : the quantity of antibodies that can neutralize D614G but fail to neutralize Omicron BA.1 at BD8 due to  
 1030 Omicron's immune escape.

Wave		Delta	Omicron	
<b>Protection against reinfection</b>	<b>Direct effect</b> (Protection absent of nAbs)	<b>Prior D614G exposure</b> (odds ratio, absent of waning)	0.76 (0.36, 1.61)	1.23 (0.63, 2.38)
		<b>Prior Beta exposure</b> (odds ratio, absent of waning)	0.47 (0.30, 0.76)	0.78 (0.50, 1.21)
		<b>Prior Delta exposure</b> (odds ratio, absent of waning)	–	0.47 (0.29, 0.76)
	<b>Mediators effect</b> (Protection from nAbs)	<b>Anti-D614G nAb</b> (odds ratio, per 10-fold increase)	0.59 (0.43, 0.83)	–
		$\Delta nAb^W$ (odds ratio, per 10-fold increase)	1.00 (0.72, 1.39)	–
		<b>Anti-BA.1 nAb</b> (odds ratio, per 10-fold increase)	–	0.73 (0.56, 0.95)
		$\Delta nAb^E$ (odds ratio, per 10-fold increase)	–	0.94 (0.76, 1.15)
	<b>Total protection</b> (relative risk compared to naïve individuals)		0.40 (0.38, 0.42)	0.70 (0.68, 0.72)
	<b>Proportion of protection mediated by nAbs</b>		37% (34%, 40%)	11% (9%, 12%)
	<b>Protection against onward transmission</b> (Odds ratio compared to naïve individuals)		0.20 (0.05, 0.72)	1.11 (0.62, 2.00)

1031

1032

1033 **Extended Data Table 3: Mediation analysis for nAbs as CoPs against Delta (ascertained by both serology and**  
 1034 **PCR) and Omicron wave infections, with a waning model for direct effect.** Average and 95% CIs are provided  
 1035 for each of the model parameters.  $\Delta nAb^W$ : the quantity of anti-D614G nAbs waned from peak level to that at BD5.  
 1036  $\Delta nAb^E$ : the quantity of antibodies that can neutralize D614G but fail to neutralize Omicron BA.1 at BD8 due to  
 1037 Omicron's immune escape.

Wave		Delta	Omicron	
<b>Protection against reinfection</b>	<b>Direct effect</b> (Protection absent of nAbs)	<b>Effect size</b> (odds ratio, absent of waning)	0.34 (0.17, 0.64)	0.29 (0.17, 0.51)
		<b>Waning half-life</b> (days)	128 (77, 261)	
	<b>Mediators effect</b> (Protection from nAbs)	<b>Anti-D614G nAb</b> (odds ratio, per 10-fold increase)	0.65 (0.49, 0.86)	–
		$\Delta nAb^W$ (odds ratio, per 10-fold increase)	1.02 (0.78, 1.36)	–
		<b>Anti-Omicron BA.1 nAb</b> (odds ratio, per 10-fold increase)	–	0.73 (0.56, 0.95)
		$\Delta nAb^E$ (odds ratio, per 10-fold increase)	–	1.01 (0.84, 1.21)
	<b>Total protection</b> (relative risk compared to naïve individuals)		0.41 (0.40, 0.43)	0.62 (0.61, 0.64)
	<b>Proportion of protection mediated by nAbs</b>		33% (30%, 35%)	11% (9%, 12%)
<b>Protection against onward transmission</b> (Odds ratio compared to naïve individuals)		0.23 (0.08, 0.71)	1.19 (0.66, 2.13)	

1038

1039

1040 **Extended Data Table 4: Mediation analysis for D614G spike binding antibody as CoPs against serologically**  
 1041 **ascertained Delta and Omicron wave infections, with a variant-specific model for direct effect.** Average and 95%  
 1042 CIs are provided for each of the model parameters.  $\Delta bAb^W$ : the quantity of D614G spike binding antibodies waned  
 1043 from peak level to that at BD5 for Delta (at BD8 for Omicron).

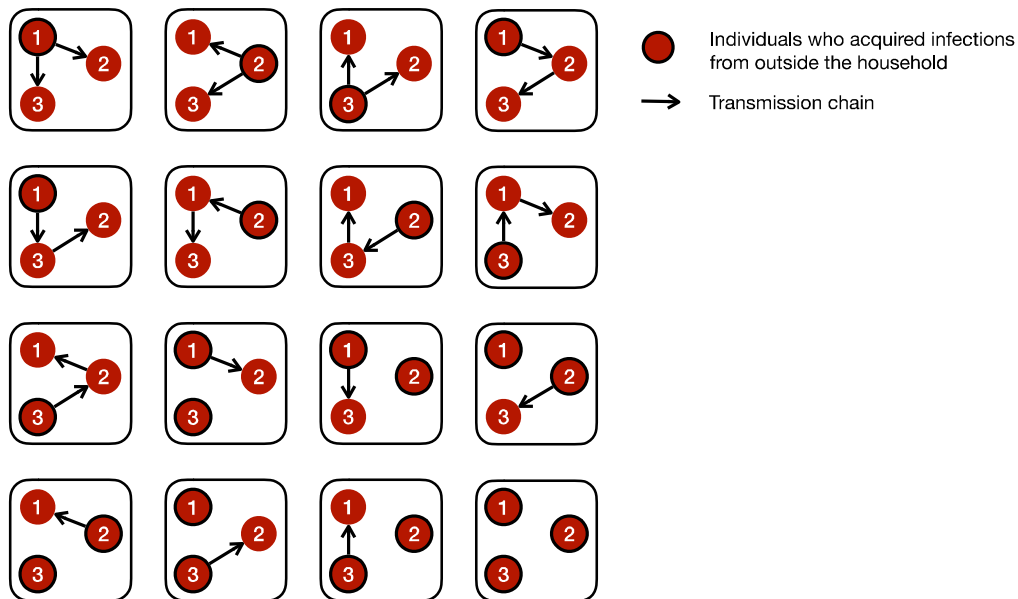
<b>Protection against reinfection</b>		Delta (serology)	Omicron (serology)
<b>Direct effect</b> (Protection absent of nAbs)	<b>Prior D614G exposure</b> (odds ratio, absent of waning)	0.60 (0.24, 1.48)	1.38 (0.67, 2.84)
	<b>Prior Beta exposure</b> (odds ratio, absent of waning)	0.51 (0.32, 0.83)	0.91 (0.58, 1.45)
	<b>Prior Delta exposure</b> (odds ratio, absent of waning)	–	0.61 (0.38, 0.97)
<b>Mediators effect</b> (Protection from nAbs)	<b>D614G binding Ab</b> (odds ratio, per 10-unit increase)	0.26 (0.12, 0.59)	0.60 (0.46, 0.77)
	<b><math>\Delta bAb^W</math></b> (odds ratio, per 10-unit increase)	1.02 (0.55, 1.91)	1.02 (0.55, 1.87)
<b>Total protection</b> (relative risk compared to naïve individuals)		0.40 (0.38, 0.42)	0.65 (0.63, 0.67)
<b>Proportion of protection mediated by spike binding Ab</b>		35% (32%, 38%)	27% (25%, 29%)
<b>Protection against onward transmission</b> (Odds ratio compared to naïve individuals)		0.22 (0.06, 0.74)	1.18 (0.65, 2.13)

1044

1045



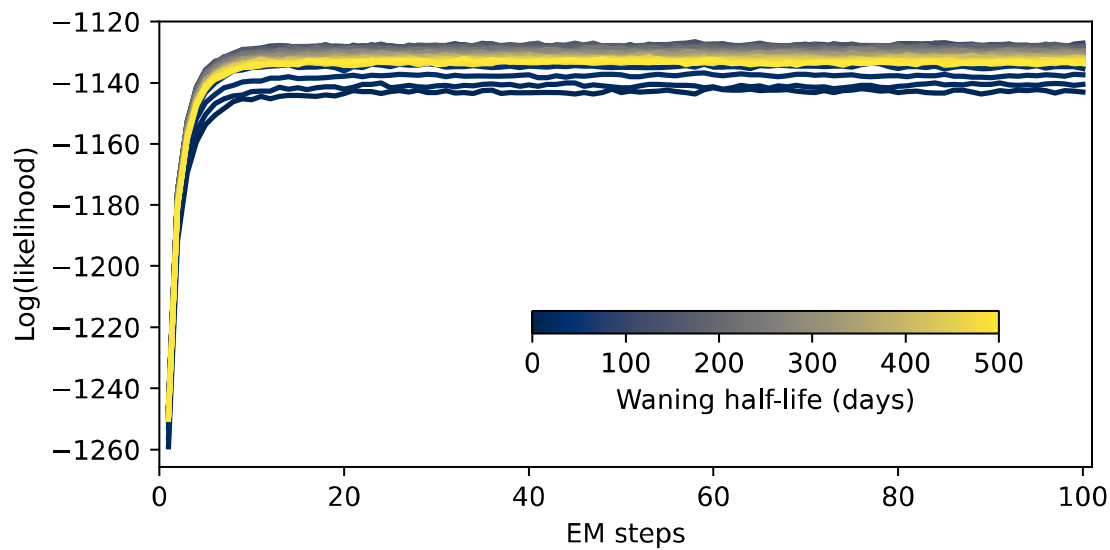
1046 **Supplementary Information**



1047

1048 **Supplementary Fig. 1:** Visualization of all 16 possible transmission chains within a household of 3 infected  
1049 individuals.

1050

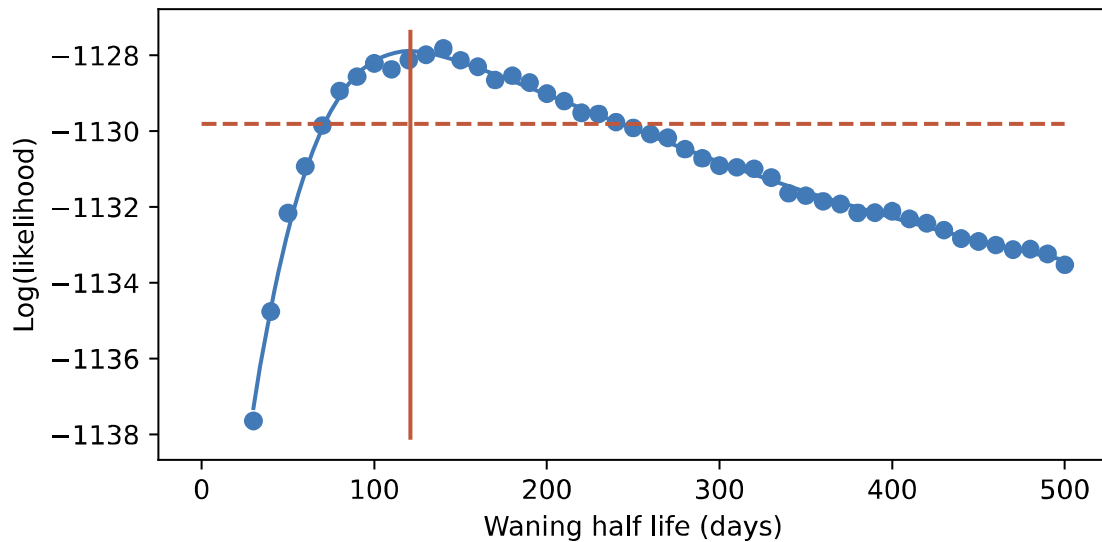


1051

1052 **Supplementary Fig. 2: The log-likelihood of the transmission model fit, as a function of the EM steps.**

1053

1054



1055

1056 **Supplementary Fig. 3: The profile log-likelihood of the transmission model over hyper-parameter of waning**

1057 **half-life.** Solid vertical line indicates the waning half-life corresponding to maximum of the profile likelihood.

1058 Dashed horizontal line represent 1.92 below the maximum profile likelihood.